DALTON
FULL PAPER

α–β Alkenyl isomerisation at diiron centres

M. Kamal Anwar,[a] **Graeme Hogarth,**[a]* **Ozan S. Senturk,**[ab] **William Clegg,**[c]
Simon Doherty[c] **and Mark R. J. Elsegood**[c]

[a] *Chemistry Department, University College London, 20 Gordon Street, London, UK WC1H 0AJ. E-mail: g.hogarth@ucl.ac.uk*
[b] *Department of Chemistry, Ege University, Bornova 35100, Izmir, Turkey. E-mail: sanli@fenfak.ege.edu.tr*
[c] *Department of Chemistry, University of Newcastle, Bedson Building, Newcastle-upon-Tyne, UK NE1 7RU. E-mail: simon.doherty@ncl.ac.uk*

Received 3rd October 2000, Accepted 1st December 2000
First published as an Advance Article on the web 12th January 2001

α-Substituted alkenyl complexes [$Fe_2(CO)_6(\mu\text{-}RC{=}CH_2)(\mu\text{-}PPh_2)$] **1a**–**1e** (R = Ph, Me, Pr^n, Bu^n or Bu^t) have been prepared *via* regioselective hydrodimetallation of primary alkynes by [$Fe_2H(CO)_7(\mu\text{-}PPh_2)$]. Thermolysis in toluene results in isomerisation to the β-substituted complexes [$Fe_2(CO)_6(\mu\text{-}HC{=}CHR)(\mu\text{-}PPh_2)$] **2a**–**2e**. Isomerisation is accelerated in the presence of a range of tertiary phosphines yielding [$Fe_2(CO)_5(PR'_3)(\mu\text{-}HC{=}CHR)(\mu\text{-}PPh_2)$] **3a**–**3j** in which the phosphine is coordinated to the σ-bound metal centre and lies *trans* to the phosphido-bridge. Addition of trimethyl phosphite to [$Fe_2(CO)_6(\mu\text{-}PhC{=}CH_2)(\mu\text{-}PPh_2)$] **1a** at 60–70 °C affords mono- and di-substituted α-alkenyl complexes [$Fe_2(CO)_5\{P(OMe)_3\}(\mu\text{-}PhC{=}CH_2)(\mu\text{-}PPh_2)$] **4** and [$Fe_2(CO)_4\{P(OMe)_3\}_2(\mu\text{-}PhC{=}CH_2)(\mu\text{-}PPh_2)$] **5** respectively. Above 100 °C, conversion into the β-substituted isomers [$Fe_2(CO)_5\{P(OMe)_3\}(\mu\text{-}HC{=}CHPh)(\mu\text{-}PPh_2)$] **6** and [$Fe_2(CO)_4\{P(OMe)_3\}_2(\mu\text{-}HC{=}CHPh)(\mu\text{-}PPh_2)$] **7** occurs cleanly. Crystallographic studies have been carried out on **1a**, [$Fe_2(CO)_6(\mu\text{-}Pr^nC{=}CH_2)(\mu\text{-}PPh_2)$] **1c**, [$Fe_2(CO)_6(\mu\text{-}HC{=}CHPh)(\mu\text{-}PPh_2)$] **2a**, [$Fe_2(CO)_5(PPh_3)(\mu\text{-}HC{=}CHPh)(\mu\text{-}PPh_2)$] **3a**, **6** and **7** and compared with related structures. Different structural characteristics are seen between isomers, β isomers being characterised by a longer Fe_π–C_β interaction and a more obtuse Fe_σ–C_α–C_β angle. The mechanisms of alkyne addition to [$Fe_2H(CO)_7(\mu\text{-}PPh_2)$] and alkenyl isomerisation have been probed using PhC_2D. Hydrodimetallation results in an equal distribution of the deuterium over both β sites in **1a**, and since they do not in exchange on the NMR timescale suggests that a radical process is operating. Thermolysis of this mixture leads to a 3 : 1 mixture of [$Fe_2(CO)_6(\mu\text{-}DC{=}CHPh)(\mu\text{-}PPh_2)$] **2a**-$d^1_\alpha$ and [$Fe_2(CO)_6(\mu\text{-}HC{=}CDPh)(\mu\text{-}PPh_2)$] **2a**-$d^1_\beta$. A mechanism for α–β alkenyl isomerisation is proposed in which oxidative additions of the *trans* (*exo*) and *cis* (*endo*) β-protons to terminal sites on the diiron centre, giving a parallel alkyne intermediate, are in competition.

Introduction

Alkenyl ligands have been proposed as key intermediates in the Fischer–Tropsch process.[1] Evidence comes from a series of labeling studies carried out by Maitlis and co-workers, which suggest that chain growth results *via* methylene insertion into the metal–carbon σ bond of a surface-bound alkenyl. This generates an allyl moiety, which subsequently undergoes isomerisation *via* a 1,3-proton shift to give a new β-substituted alkenyl. As a result of this proposal, the chemistry of alkenyl ligands has been studied at a variety of metal centres, emphasis being placed on carbon–carbon bond forming reactions.[2–4]

The proposed surface-bound alkenyl ligands are monosubstituted. Such species can adopt three possible isomeric forms, shown for a binuclear centre as **I–III**, with the substituent on either the α- (**I**) or β- (**II**,**III**) carbon, the latter being either *trans* (**II**) or *cis* (**III**) to the metal centre. At a binuclear centre, interconversion of *cis* and *trans* β isomers (**II**,**III**) has been noted in a number of instances. For example, Nubel and Brown[5] have shown that *cis*-[$Re_2(CO)_8(\mu\text{-}H)(\mu\text{-}HC{=}CHR)$] (R = Me, Et) converts into the thermodynamically stable *trans* isomers both thermally and photochemically (eqn. 1). While the thermal transformation is clean, upon photolysis a photostationary equilibrium state results. Similarly, we have previously shown[6] that photolysis of the disubstituted alkenyl complex [$Fe_2(CO)_4(\mu\text{-}RC{=}CHR)(\mu\text{-}PPh_2)(\mu\text{-}dppm)$] (R = CO_2Me), in which the ester groups lie *cis* to one another, results in isomerisation at the β-carbon, a process which is reversed thermally (eqn. 2).

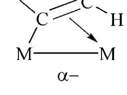

α-
(I)

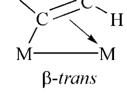

β-*trans*
(II)

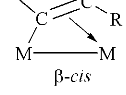

β-*cis*
(III)

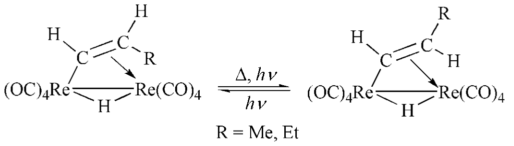

(1)

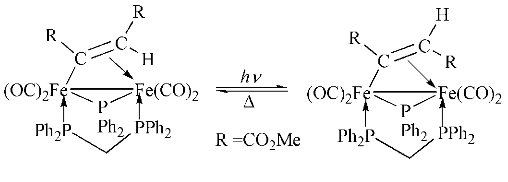

(2)

Until recently there was little evidence for α–β isomerisation in alkenyl complexes; that is, conversion of **I** to **II**,**III**. On the basis of NMR results, Knox and co-workers[7] have suggested that propenyl cations $[Fe_2Cp_2(CO)_2(\mu\text{-}CO)(\mu\text{-}HC{=}CHMe)]^+$ and $[Fe_2Cp_2(CO)_2(\mu\text{-}CO)(\mu\text{-}MeC{=}CH_2)]^+$ may be in equilibrium, however, this could not be shown conclusively. In the same paper a reference to unpublished results[8] suggests that α–β propenyl isomerisation occurs in dimolybdenum cations. Thus, protonation of the μ-allene complex $[Mo_2Cp_2(CO)_4(\mu\text{-}H_2C{=}C{=}CH_2)]$ affords β-substituted $[Mo_2Cp_2(CO)_4(\mu\text{-}HC{=}CHMe)]^+$ rather than the α isomer which would be expected to be formed initially. Similar evidence for α–β propenyl isomerisation comes from our work on reactions of $[Fe_2(CO)_4(\mu\text{-}H)(\mu\text{-}CO)(\mu\text{-}PR_2)(\mu\text{-}dppm)]$ (R = Ph or Cy) with allene, which result in a mixture of α- and β-propenyl complexes.[9,10]

A number of synthetic routes to alkenyl complexes are known, one widely utilised being the hydrometallation of alkynes. Here, primary alkynes can give either α- or β-substituted isomers depending upon the regioselectivity of the insertion, with the former generally predominating since they result from Markovnikov addition. Carty and co-workers have previously reported that hydrodimetallation of PhC_2H by $[Fe_2H(CO)_7(\mu\text{-}PPh_2)]$ afforded a mixture of α-$[Fe_2(CO)_6(\mu\text{-}PhC{=}CH_2)(\mu\text{-}PPh_2)]$ **1a** and β-$[Fe_2(CO)_6(\mu\text{-}HC{=}CHPh)(\mu\text{-}PPh_2)]$ **2a** substituted phenylethenyl complexes in a 4 : 1 ratio.[11] As part of our work on σ–π alkenyl reactivity and fluxionality at the diiron centre,[9,10,12–14] we have used **1a** as an entry into dppm-bridged alkenyl complexes since the diphosphine ligand acts as a convenient NMR probe of this process.[12] In repeating its synthesis we found that room temperature work-up gave only the α isomer $[Fe_2(CO)_6(\mu\text{-}PhC{=}CH_2)(\mu\text{-}PPh_2)]$ **1a**, as shown by ^1H NMR spectroscopy. However, if the temperature is raised to 110 °C, then α–β isomerisation occurs cleanly, a process which is accelerated in the presence of a phosphine. Herein we follow up on our preliminary communication[15] concerning phenylethenyl complexes to show that α–β isomerisation is a general process in these complexes and that ground-state differences in the binding of the alkenyl ligand in α- and β-substituted complexes may be the origin of different thermodynamic stabilities.

Results and discussion

Synthesis of α-alkenyl complexes $[Fe_2(CO)_6(\mu\text{-}RC{=}CH_2)(\mu\text{-}PPh_2)]$ 1

Hydrodimetallation of primary alkynes by $[Fe_2H(CO)_7(\mu\text{-}PPh_2)]$ leads to regioselective formation of α-substituted alkenyl complexes $[Fe_2(CO)_6(\mu\text{-}RC{=}CH_2)(\mu\text{-}PPh_2)]$[11,16] **1a–1e**, while with PhC_2Me a single isomer, namely, $[Fe_2(CO)_6(\mu\text{-}PhC{=}CHMe)(\mu\text{-}PPh_2)]$[16] **1f** also results. All are the expected Markovnikov type addition products. Only with propyne a small amount (≈ 10%) of the β isomer $[Fe_2(CO)_6(\mu\text{-}HC{=}CHMe)(\mu\text{-}PPh_2)]$ **2b** was formed. Characterisation of **1a**–**1e** was straightforward and based on ^1H NMR spectra, each displaying two signals between δ 3.2 and 2.0 assigned to inequivalent β-protons of the alkenyl ligand. Carty and co-workers[11] had previously noted high regioselectivity in reactions of alkynes and diynes with $[Fe_2H(CO)_7(\mu\text{-}PPh_2)]$, although for some primary alkynes (R = Ph, $SiMe_3$ or $C_6H_4C_2Ph$) they reported the formation of mixtures of α- and β-substituted isomers.

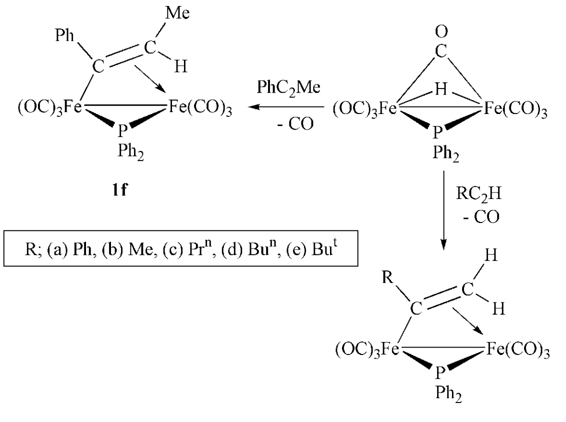

Hydrometallation reactions generally proceed in a *cis* fashion *via* initial coordination of the alkyne to the metal centre followed by *cis* addition of the hydride *via* a planar transition state.[17–19] In a number of instances *trans* addition products have been isolated[20–22] and this is accounted for either by postulating rapid isomerisation of the initially formed *cis* addition product,[20] or a free-radical pathway.[21,22] In order to probe the hydrodimetallation further we examined the reaction with PhC_2D. Somewhat surprisingly, this afforded $[Fe_2(CO)_6(\mu\text{-}PhC{=}CHD)(\mu\text{-}PPh_2)]$ **1a**-d^1 as a 1 : 1 mixture of *cis* and *trans* alkyne addition products.

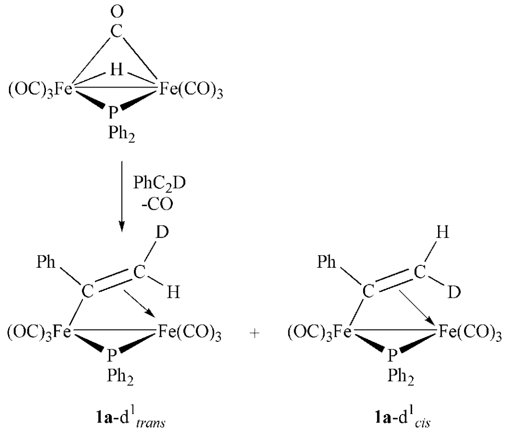

Initially this was considered to result from the interconversion of the two β-proton sites in complex **1a** and such a process has been shown to occur in related triosmium complexes in the presence of pyridine.[23] However, a ^1H NOESY spectrum clearly showed that this was not the case, implying that either *cis*–*trans* isomerisation occurs during the reaction or a free-radical pathway is operative. While we cannot definitely rule out the former, the observation of a 1 : 1 mixture (within experimental error) points strongly towards the latter. The most likely source of free radicals is homolytic cleavage of the iron–iron bond and it may be that the phosphido-bridge acts to hold the two metal centres together during this process. However, Baker *et al.*[24] have reported that oxidation of $Na[Fe_2(CO)_{7/8}(\mu\text{-}PPh_2)]$ by ferrocenium affords stable paramagnetic 33-electron $[Fe_2(CO)_7(\mu\text{-}PPh_2)]$ and we cannot discount the possibility that this radical is generated during our procedure.

α–β Alkenyl isomerisation: synthesis of β-alkenyl complexes $[Fe_2(CO)_6(\mu\text{-}HC{=}CHR)(\mu\text{-}PPh_2)]$ 2a–2e

Heating toluene solutions of complexes **1a**–**1e** at 110 °C for 45 min to 4 h resulted in isomerisation to the β-alkenyl complexes $[Fe_2(CO)_6(\mu\text{-}HC{=}CHR)(\mu\text{-}PPh_2)]$ **2a**–**2e**. Yields varied [**2a** (R = Ph), 95%; **2c** (R = Pr^n), 28%] as did reaction times. Thus, formation of **2d** (R = Bu^n) and **2e** (R = Bu^t) required 45 min, **2a** (R = Ph) 1 h, while conversion of **1b** (R = Me) took 4 h. Characterisation was made on the basis of ^1H NMR spectra, the newly generated α-proton appearing as a low-field doublet

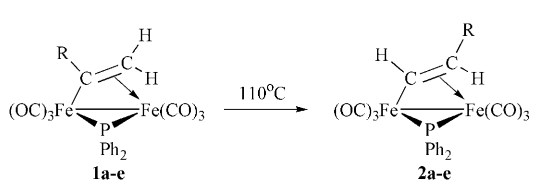

of doublets between δ 8.9 and 7.9. Monitoring by ^{1}H NMR spectroscopy showed that the transformations of **1a** and **1e** were first order in complex concentration.

Acceleration of α–β alkenyl isomerisation by tertiary phosphines: synthesis of [$Fe_2(CO)_5(PR'_3)(\mu$-HC=CHR)(μ-PPh_2)] 3a–3j

Heating toluene solutions of complex **1a** (R = Ph) and a range of tertiary phosphines at 110 °C resulted in the rapid (≈ 10 min) formation of the phosphine-substituted β-alkenyl complexes [$Fe_2(CO)_5(PR'_3)(\mu$-HC=CHPh)(μ-PPh_2)] **3a**–**3g**. In no instance was there any evidence for formation of the α-alkenyl isomer. Characterisation was straightforward, in each case the ^{1}H NMR spectrum containing a characteristic low-field doublet of doublet of doublets for the α-proton with couplings of approximately 6 Hz to the phosphido-bridge, 13 Hz to the β-proton and 28 Hz to the phosphine ligand. The latter suggested that the phosphine was coordinated to the σ-bound iron centre and this was confirmed by X-ray crystallography (see later). In the ^{31}P NMR spectra only one isomer was detected, appearing as a pair of low- and high-field doublets assigned to the phosphido-bridge and phosphine respectively, the coupling constant of around 94 Hz being indicative of a *trans* arrangement of phosphorus atoms. All were temperature independent indicating that the two phosphorus centres are static on the NMR timescale as is the alkenyl ligand. In a separate experiment, heating a toluene solution of **2a** and PPh_3 at 110 °C for 10 min resulted in quantitative formation of [$Fe_2(CO)_5(PPh_3)(\mu$-HC=CHPh)(μ-PPh_2)] **3a** showing that phosphine substitution of the β-alkenyl complexes is facile. Further phosphine substitution did not occur even under forcing conditions. Thus, refluxing a toluene solution of **3a** with a large excess of PPh_3 for over one week resulted only in the isolation of starting materials.

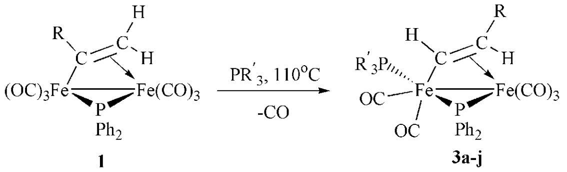

1 **3a-j**

R = Ph, R'; (a) Ph; (b) *p*-tolyl; (c) *m*-tolyl; (d) *p*-FC_6H_4; (e) CH_2CH_2CN; (f) Me
R = Ph, ER'$_3$; (g) PPh_2Me; (h) $AsPh_3$; (i) R = Bu^t, R' = Ph; (j) R = Me, R' = Ph

Alkenyl isomerisation in complex **1a** was also effected in the presence of $AsPh_3$ leading to the formation of [$Fe_2(CO)_5(AsPh_3)(\mu$-HC=CHPh)(μ-PPh_2)] **3h** in 14% yield. Further, the course of the reaction of **1a** with tolylphosphines was dependent upon the position of methyl substitution. Thus, while $P(C_6H_4Me$-*p*$)_3$ and $P(C_6H_4Me$-*m*$)_3$ gave the expected phosphine-substituted β-alkenyl complexes **3b** and **3c** respectively after 10 min, the more sterically demanding $P(C_6H_4Me$-*o*$)_3$ and likewise PCy_3 simply gave **2a** after 1 h.

Thermolysis of complex **1d** (R = Bu^t) and PPh_3 resulted in a significant rate enhancement (from 45 to 10 min) leading to formation of [$Fe_2(CO)_5(PPh_3)(\mu$-HC=CHBu^t)(μ-PPh_2)] **3i** in 57% yield. With **1b** (R = Me) and PPh_3 rate enhancement was also observed (from 4 to 1 h), [$Fe_2(CO)_5(PPh_3)(\mu$-HC=CHMe)(μ-PPh_2)] **3j** being formed cleanly (93%). However, when this reaction was stopped after 30 min a second product was clearly seen by NMR, formulated as the phosphine-substituted α-alkenyl complex [$Fe_2(CO)_5(PPh_3)(\mu$-MeC=CH_2)(μ-PPh_2)] **3j′**. In the ^{1}H NMR spectrum the two β-protons are seen at δ 2.29 (dd, *J* 7.9, 3.0, H_{cis}) and 2.07 (ddd, *J* 15.3, 6.7, 3.0 Hz, H_{trans}). Comparison with the ^{1}H NMR spectrum of **2b** shows that the only coupling of the β-protons to PPh_3 is that of 6.7 Hz to H_{trans}. In the ^{31}P NMR spectrum two doublets are observed at δ 168.5 and 64.1, the phosphorus–phosphorus coupling constant of 63.4 Hz suggesting that the phosphorus containing ligands lie *cis* to one another. On the basis of these data, and in comparison with data for isomer (A) of the related complex [$Fe_2(CO)_5\{P(OMe)_3\}(\mu$-PhC=$CH_2$)($\mu$-$PPh_2$)] **4** (see later), we assign the structure shown in which the phosphine is coordinated to the π-bound iron centre and lies *trans* to the metal–metal bond. Heating the mixture of **1b**, **3j**, **3j′** and PPh_3 further resulted in clean conversion to **3j** showing that **3j′** is an intermediate in the transformation. These results suggest that, in all cases, phosphine substitution is rate-determining and that α–β alkenyl isomerisation occurs rapidly for the phosphine-substituted α-alkenyl complexes.

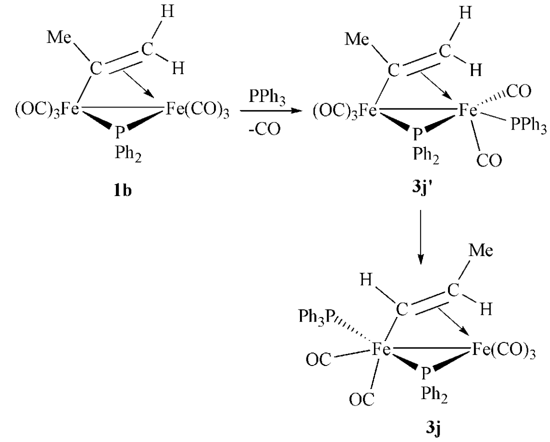

1b **3j'** **3j**

Synthesis of α-alkenyl phosphite complexes [$Fe_2(CO)_5\{P(OMe)_3\}(\mu$-PhC=$CH_2$)($\mu$-$PPh_2$)] 4 and [$Fe_2(CO)_4\{P(OMe)_3\}_2(\mu$-PhC=$CH_2$)($\mu$-$PPh_2$)] 5

Heating a toluene solution of complex **1a** and $P(OMe)_3$ at 65–75 °C resulted in formation of both mono- and di-substituted phosphite derivatives [$Fe_2(CO)_5\{P(OMe)_3\}(\mu$-PhC=$CH_2$)($\mu$-$PPh_2$)] **4** and [$Fe_2(CO)_4\{P(OMe)_3\}_2(\mu$-PhC=$CH_2$)($\mu$-$PPh_2$)] **5**

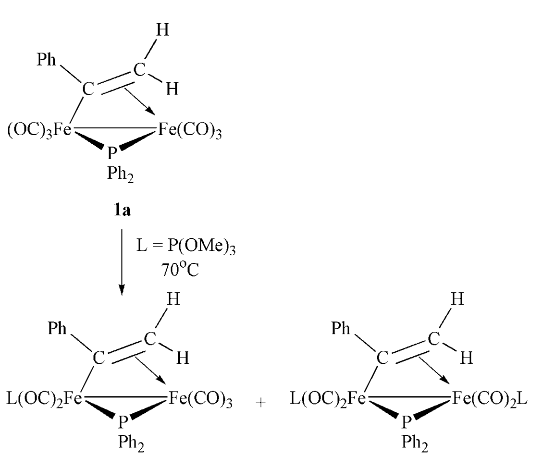

1a **4** **5**

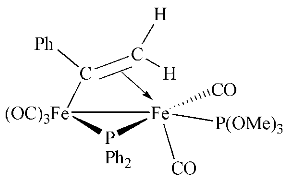
4 (A)

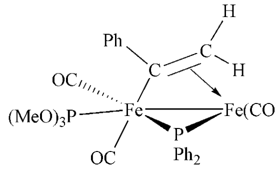
4 (B)

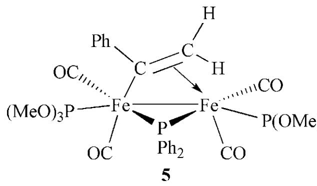
5

isolated in 47 and 34% yields respectively. A ^{1}H NMR spectrum of the crude reaction mixture revealed that no α–β isomerisation had occurred under these conditions.

Complex **4** was shown by ^{31}P NMR to be a 2 : 1 mixture of isomers at 213 K. Both appeared as two sharp doublets; one at δ 186.6 and 165.0 (J 70.2 Hz) due to the major isomer (A), the and other at δ 188.1 and 152.5 (J 52.7 Hz) due to minor isomer (B). The magnitude of the phosphorus–phosphorus coupling constants suggests that in both isomers the phosphite lies *cis* to the phosphido-bridge, as a *trans* orientation is expected to have a much larger coupling constant. Further, on the basis that the β-protons of isomer (A) couple with the phosphite (J_{PH} = 3.3 Hz), while those of isomer (B) do not, we propose that (A) has the phosphite coordinated to the π-bound iron centre, while in (B) it is located on the σ-bonded metal.

Disubstituted complex **5** exists as a single isomer which appears in the ^{31}P NMR spectrum at 213 K as a pair of sharp doublets at δ 189.8 (J 47.0) and 189.1 (J 71.6 Hz) assigned to the inequivalent phosphite ligands, and a broad doublet of doublets at δ 145.9 assigned to the phosphido-bridge. Given the similarity of these coupling constants to those of the two isomers of **4** it seems reasonable to suggest that similar sites are occupied; that is, one on each iron centre with both lying *cis* to the phosphido-bridge. While we cannot be certain, we favour coordination at the sites *trans* to the metal–metal bond. This is supported by the observation that in the ^{13}C NMR spectrum neither C_α nor C_β shows a significant coupling to either phosphite ligand. Also, in the related thiolate-bridged complex $[Fe_2(CO)_4\{P(OMe)_3\}_2(\mu\text{-}SBu^t)(\mu\text{-}PhC{=}CH_2)]$[25] the two phosphite ligands have been shown by X-ray crystallography to occupy sites *trans* to the metal–metal bond.

Phosphite accelerated α–β alkenyl isomerisation: synthesis of $[Fe_2(CO)_5\{P(OMe)_3\}(\mu\text{-}HC{=}CHPh)(\mu\text{-}PPh_2)]$ 6 and $[Fe_2(CO)_4\{P(OMe)_3\}_2(\mu\text{-}HC{=}CHPh)(\mu\text{-}PPh_2)]$ 7

Heating a toluene solution of complex **4** at 100 °C resulted in quantitative conversion into the β-alkenyl isomer $[Fe_2(CO)_5\{P(OMe)_3\}(\mu\text{-}HC{=}CHPh)(\mu\text{-}PPh_2)]$ **6** within 10 min, and under the same conditions **5** cleanly afforded $[Fe_2(CO)_4\{P(OMe)_3\}_2(\mu\text{-}HC{=}CHPh)(\mu\text{-}PPh_2)]$ **7**. In a separate experiment, approximately equal amounts of **4** and **5** were warmed to 100 °C in d^8-toluene whilst monitoring by ^{31}P NMR spectroscopy. Below 90 °C no significant conversion of either into the β-isomer occurred, however at 100 °C both **6** and **7** grew in at approximately equal rates.

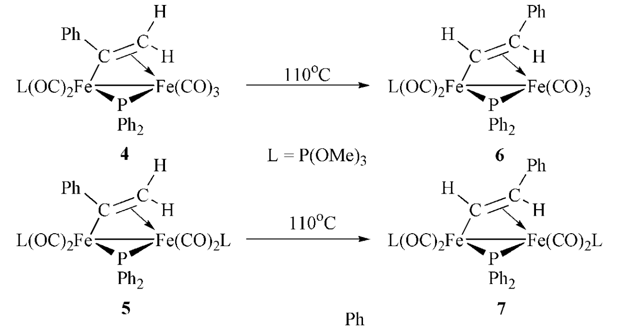

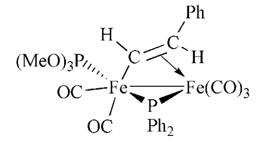

6

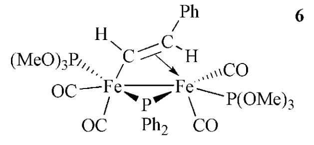

7 (A)

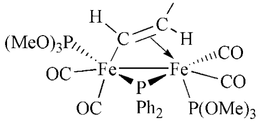

7 (B)

Like the α isomers, both complexes **6** and **7** have highly temperature dependent NMR spectra. At low temperature (223 K) the ^{31}P NMR spectrum of **6** shows a pair of doublets at δ 182.6 and 177.7, the phosphorus–phosphorus coupling constant of 154.7 Hz clearly indicating that the two phosphorus atoms lie *trans* to one another. In the ^{1}H NMR spectrum at the same temperature the α-proton is seen at δ 8.73 (ddd, J 31.8, 12.7, 8.1 Hz). The large coupling constant (J_{PH} 31.8 Hz) is that to the phosphite ligand, suggesting that substitution has occurred at the σ-bound iron centre. This conclusion was later confirmed by X-ray crystallography.

Disubstituted complex **7** exists at low temperature as a mixture of two isomers (A : B) in an approximate 6 : 1 ratio. At 223 K the ^{31}P NMR spectrum clearly shows this, the major isomer (A) being seen as a pair of doublets at δ 188.6 (J 145.7) and 180.3 (J 59.8 Hz) assigned to the phosphites, while the phosphido-bridge appears as a doublet of doublets at δ 165.4. The minor isomer (B) has a similar spectrum, with two phosphite resonances at δ 196.8 (d, J 45.5) and 181.0 (d, J 150.7 Hz) and the phosphido-bridge at δ 159.0 (dd, J 150.7, 45.0 Hz). In the ^{1}H NMR spectrum (223 K) two low-field resonances are apparent at δ 8.74 (ddd, J 30.2, 13.0, 8.1 Hz) and 8.63 (br) assigned to isomers (A) and (B) respectively. Resonances due to (B) are not well resolved and often overlap with those of the more abundant (A) making assignment of this isomer difficult. Assignment of the major isomer (A) was made on the basis of a crystallographic study (see later). The phosphite at the σ-bound metal centre lies *trans* to the phosphido-bridge, while that at the π-bound iron lies *trans* to the metal–metal vector. On the basis of this assignment, and since the two isomers interconvert, we tentatively assign isomer (B) as that having the same phosphite orientation at the σ-bound centre but with the phosphite at the π-bound centre lying *trans* to the β-carbon of the alkenyl ligand.

Mechanism of α–β alkenyl isomerisation

While α–β alkenyl isomerisation could occur *via* a direct 1,2-proton shift, we disfavour such a process on the grounds that it is difficult to rationalise the rate acceleration by phosphines and phosphites. Knox and co-workers[7] have suggested previously that it probably involves a temporary hydrogen shift to a bonding site on the dimetal centre. If we accept this supposition we still need to consider whether both β-hydrogens undergo addition or if the process is selective. In α isomers **1** the *trans* proton lies *exo* to the phosphido-bridge, while the *cis* proton lies *endo* to it. From the crystal structures of both **1a** and **1c** it is seen that the *endo* proton lies closer than the *exo* proton to the π-bound metal [**1a** (**1c**), Fe_π–H_{exo} 2.814 (2.791), Fe_π–H_{endo} 2.563 (2.657) Å], which suggests that *cis* (*endo*) proton addition might be favourable.

Some insight was gained from a deuterium labeling study. At 110 °C the 1 : 1 *cis–trans* mixture of $[Fe_2(CO)_6(\mu\text{-}PhC{=}CHD)(\mu\text{-}PPh_2)]$ **1a**-d^1 was transformed into $[Fe_2(CO)_6(\mu\text{-}DC{=}CHPh)(\mu\text{-}PPh_2)]$ **2a**-d$^1_\alpha$ and $[Fe_2(CO)_6(\mu\text{-}HC{=}CDPh)(\mu\text{-}PPh_2)]$ **2a**-d$^1_\beta$

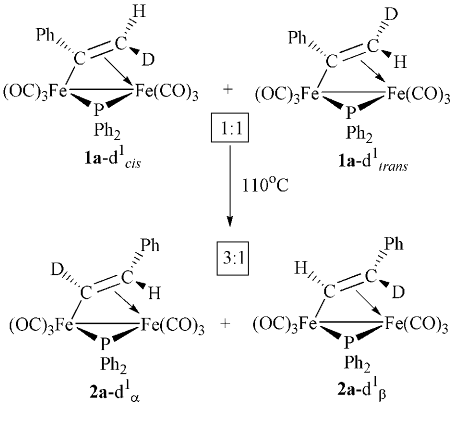

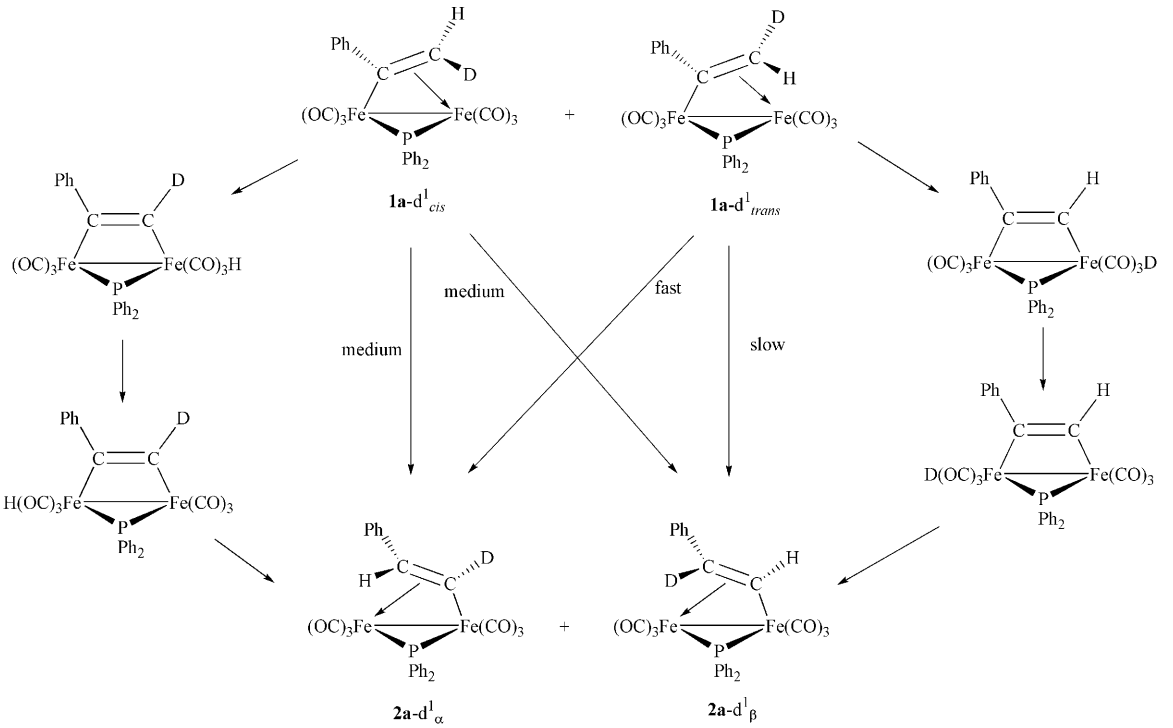

Scheme 1

in a 3 : 1 ratio and this remained constant upon further heating. The latter observation confirms that the alkenyl protons in β-substituted complexes, like those in the α isomers, do not exchange. Thus, the redistribution of deuterium does not occur in either of the ground states.

This result is difficult to interpret unambiguously but, assuming that the β-protons do not interconvert (as shown by NMR and supported by literature precedent), then it does show that *both* of the β-protons undergo transfer. For example, if only addition of the *trans* (*exo*) proton occurred then complex **1a**-d$^{1}_{cis}$ would give **2a**-d$^{1}_{\alpha}$ and **1a**-d$^{1}_{trans}$ would give **2a**-d$^{1}_{\beta}$ exclusively, and while their rates of formation might be different (as a result of the different rates of C–H *vs.* C–D addition) the 1 : 1 ratio should be maintained. The same follows for addition of the *cis* (*endo*) proton and it is only a combination of the two, together with a kinetic isotope effect, which can account for the observed 3 : 1 ratio.

A further point for consideration is whether proton addition occurs to a bridging or terminal site on the diiron centre. In order to maintain the EAN of 34 electrons, a parallel 2-electron donor alkyne intermediate seems likely to be generated. We assume that the phosphido-bridge and hydrocarbyl fragments retain their relative *cis* disposition throughout and note that in related zwitterionic diiron complexes of this type this is the case.[26] Oxidative addition of either proton might occur to a terminal site but it is only the *trans* (*exo*) proton which can add across the metal–metal bond as the phosphido-bridge blocks the site of addition of the *cis* (*endo*) proton. Addition to a terminal site necessitates proton mobility to either the bridging site or a terminal site on the more sterically encumbered iron atom. While we cannot differentiate unambiguously between these possible reaction pathways, given that both protons must be able to undergo addition, we favour initial addition to a terminal site. The observed ratio of isotopomers can then be rationalised in terms of a difference in the rates of addition of the two protons combined with a kinetic isotope effect. Scheme 1 shows this based on the assumption that the closer *cis* (*endo*) proton adds faster than the more distant *trans* (*exo*) proton. For **1a**-d$^{1}_{trans}$, oxidative addition of the *cis* proton should proceed rapidly to generate **2a**-d$^{1}_{\alpha}$, while in contrast addition of the *trans* deuterium will be slow, based on a kinetic isotope effect and the unfavourable addition site. Thus, **1a**-d$^{1}_{trans}$ should afford **2a**-d$^{1}_{\alpha}$ exclusively. In **1a**-d$^{1}_{cis}$ the deuterium is now in the preferred position for oxidative addition and thus addition of the *trans* proton becomes competitive. The observed 3 : 1 ratio for **2a**-d$^{1}_{\alpha}$: **2a**-d$^{1}_{\beta}$ can be accounted for if the rates of conversion of **1a**-d$^{1}_{cis}$ into both are approximately equal.

Acceleration of α–β alkenyl isomerisation in the presence of phosphines and phosphites may simply be a consequence of the increased basicity of the metal upon substitution leading to an increase in the rate of oxidative addition. Phosphites are poorer donors than phosphines and affect the rate to a lesser extent. It is difficult to assess the extent of the rate acceleration as a function of the phosphine, as it is undoubtedly carbonyl substitution that is rate-limiting. Detection of the intermediate $[Fe_2(CO)_5(PPh_3)(\mu\text{-}MeC{=}CH_2)(\mu\text{-}PPh_2)]$ **3j**′ by NMR and isolation of $[Fe_2(CO)_5\{P(OMe)_3\}(\mu\text{-}PhC{=}CH_2)(\mu\text{-}PPh_2)]$ **4** shows that the preferred site of ligand substitution for α-alkenyl complexes **1** lies *cis* to the phosphido-bridge, probably at the π-bound iron centre. The former may give rise to unfavourable steric interactions in the ground state which are relieved upon α–β alkenyl isomerisation as the phosphido-bridge and phosphine adopt a relative *trans* configuration. If the phosphine is too sterically encumbered then coordination to the diiron centre cannot occur and no rate acceleration is found.

The rate of alkenyl isomerisation is sensitive to the nature of the alkenyl substituent being fastest for the large groups (R = Ph, Bu^n or Bu^t) and slowest for the small methyl substituent. This suggests that there may be unfavourable steric interactions between the phosphido-bridge and alkenyl substituent in the α isomers which are relieved upon oxidative addition of a β-proton. The nature of these is difficult to see and certainly none is apparent from the crystal structure determinations.

Oxidative addition of methyl to the diiron centre: synthesis of $[Fe_2(CO)_6(\mu\text{-}HC{=}CHCH_2Ph)(\mu\text{-}PPh_2)]$ 2f

Thermolysis of $[Fe_2(CO)_6(\mu\text{-}PhC{=}CHMe)(\mu\text{-}PPh_2)]$ **1f** at 110 °C for 1 h resulted in the isolation of a new alkenyl complex $[Fe_2(CO)_6(\mu\text{-}HC{=}CHCH_2Ph)(\mu\text{-}PPh_2)]$ **2f** in 42% yield. The mass spectrum clearly showed that isomerisation had occurred. In the ^{1}H NMR spectrum the newly generated α-proton appeared at δ 8.10 (dd, J 12.4, 6.5 Hz) and the β-proton as a quintet at δ 3.34 (J 6.5 Hz), being coupled approximately equally to the phosphido-bridge, α-proton and the two inequivalent benzylic hydrogens. The latter appeared as a broad singlet at room temperature, but upon cooling to 233 K separated into a pair of distinct signals at δ 3.35 (dd, J 14.0, 7.3) and 2.66 (dd, J 14.0, 7.0 Hz).

Although its mode of formation is unclear, a plausible route is shown in Scheme 2. Addition of the *cis* (*endo*) proton to the metal centre potentially leads to the formation of isomeric [$Fe_2(CO)_6(\mu\text{-}MeC{=}CHPh)(\mu\text{-}PPh_2)$]. While minor unidentified products were isolated from the reaction this was not one of them. It may be that **1f** is thermodynamically preferred over this isomer and that addition of the *cis* proton is reversible. In the absence of a *trans* (*exo*) β-proton, addition of one of the methyl protons to the metal centre would give a dimetallacyclopentene complex. Related diiron phosphido-bridged species have recently been characterised.[27] A 1,3-phenyl migration to the methylene to give a benzyl-substituted vinylidene, followed by proton transfer to the metal-bound carbon, would generate the observed β-alkenyl complex. Carrying out the thermolysis of **1f** in the presence of PPh_3 failed to yield any characterisable products.

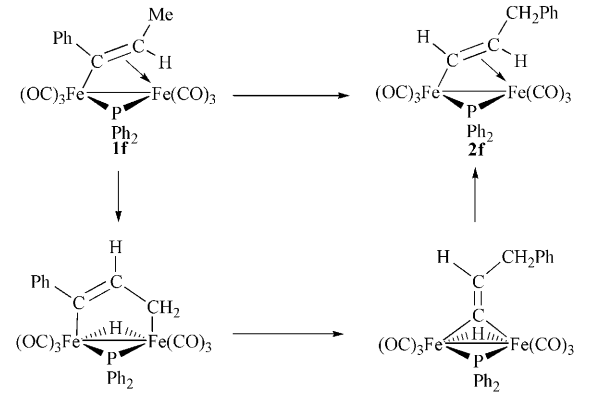

Scheme 2

Crystallographic studies

In order to probe ground-state differences between α- and β-alkenyl complexes, crystallographic studies were carried out on [$Fe_2(CO)_6(\mu\text{-}PhC{=}CH_2)(\mu\text{-}PPh_2)$] **1a**, [$Fe_2(CO)_6(\mu\text{-}Pr^nC{=}CH_2)(\mu\text{-}PPh_2)$] **1c**, [$Fe_2(CO)_6(\mu\text{-}HC{=}CHPh)(\mu\text{-}PPh_2)$] **2a**, [$Fe_2(CO)_5(PPh_3)(\mu\text{-}HC{=}CHPh)(\mu\text{-}PPh_2)$] **3a**, [$Fe_2(CO)_5\{P(OMe)_3\}(\mu\text{-}HC{=}CHPh)(\mu\text{-}PPh_2)$] **6** and [$Fe_2(CO)_4\{P(OMe)_3\}_2(\mu\text{-}HC{=}CHPh)(\mu\text{-}PPh_2)$] **7**. Figs. 1–3 give perspective views of each of the molecules, while the results are summarised in Table 1. For **7** there are three independent molecules in the unit cell and data are given for each.

In all, the diiron centre is bridged by both phosphido and alkenyl ligands, the latter binding in a σ,π manner. In complex **3a** the PPh_3 ligand is coordinated to the σ-bound iron centre ligand and lies *trans* to the phosphido-bridge [P(1)–Fe(1)–P(2) 162.08(5)°], while in **6** the phosphite coordinates in a similar fashion [P(1)–Fe(2)–P(2) 157.83(6)°]. All three independent molecules of **7** have the same general structure, that is with the phosphite at the σ-bound metal centre lying *trans* to the phosphido-bridge [P–Fe–P 157.86(14)–166.81(13)°] and the phosphite at the π-bound centre lies *cis* to the phosphido-bridge [P–Fe–P 97.39(12)–100.24(13)°] and *trans* to the metal–metal bond [P–Fe–Fe 150.70(11)–152.31(12)°].

Gross structural details of the $Fe_2(\mu\text{-}PPh_2)(\mu\text{-alkenyl})$ core for all crystallographically characterised complexes are similar. The two bridging ligands lie *cis* to one another, with the α-carbon of the alkenyl group *exo* and the β-carbon *endo* to the phosphido-bridge, while, in both α and β isomers, the alkenyl substituent also adopts an *exo* configuration. The iron–iron bond length varies over a short-range (0.032 Å), being longest [2.6427(8) Å] in **3a** and shortest in molecule C of **7** [2.611(2) Å]. However, on closer inspection a number of more subtle and potentially important differences appear between α- and β-substituted complexes (Table 1). These become evident when considering two parameters, ΔC_α and ΔFe_π, defined as {(Fe_π–C_α) − (Fe_σ–C_α)} and {(Fe_π–C_α) − (Fe_π–C_β)} respectively. ΔC_α is a measure of how symmetrically the α-carbon is bound to the diiron centre. For α-substituted complexes, ΔC_α is around 0.10 Å, while β isomers are characterised by values of 0.12 Å. A bigger difference is seen in ΔFe_π, where α isomers have values around 0.06 Å, and β isomers nearer 0.14 Å. Thus, in β isomers, binding of the α-carbon to the diiron centre and the carbon–carbon double bond of the alkenyl ligand to iron are more asymmetric than in the α isomers. The origin of the larger values of ΔFe_π for β isomers is the elongation of the Fe_π–C_β bond. This is further reflected in the Fe_σ–C_α–C_β bond angle which is more acute in α [**1a**, 121.3(4); **1c**, 124.4(8)°] *versus* β isomers [128.9(3)–133.4(8)°]. A test of the significance of these regular, but small, differences comes with the three independent molecules of **7**. While the parameters do vary, there is no overlap with the values found for α isomers. Isomers **1a** and **2a** differ only in the mode of substitution at the alkenyl ligand. Here the difference in all three parameters is consistent with the general trend; ΔC_α (**1a**, 0.102; **2a**, 0.123 Å), ΔFe_π (**1a**, 0.056; **2a**, 0.150 Å) and Fe_σ–C_α–C_β [**1a**, 121.3(4); **2a**, 128.9(3)°].

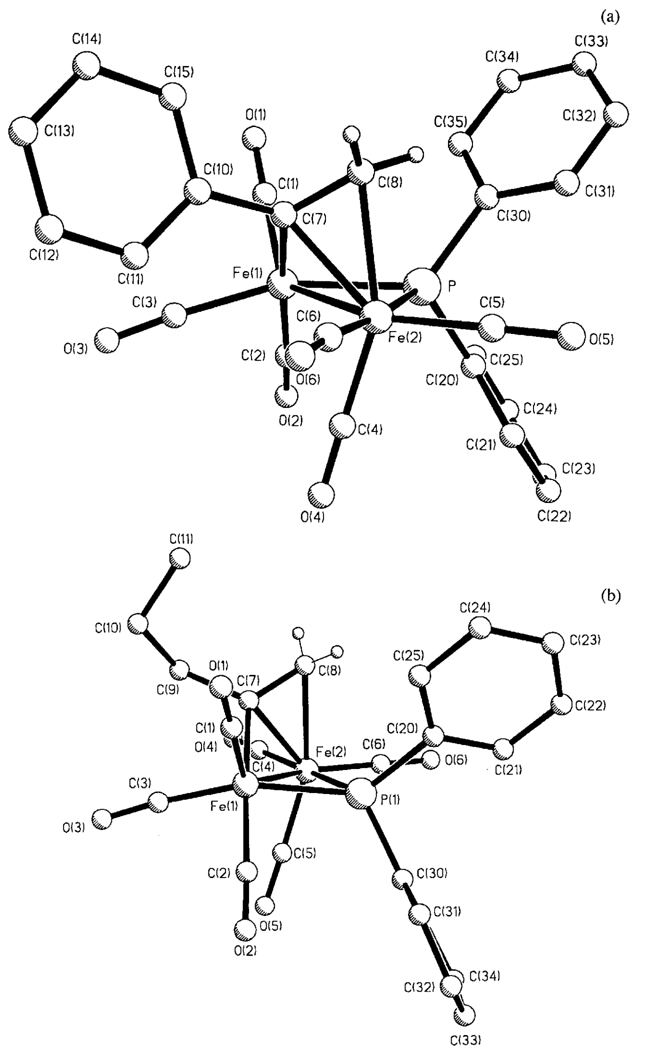

Fig. 1 Molecular structures of (a) complex **1a** and (b) **1c**.

We have previously crystallographically characterised isomeric [$Fe_2(CO)_4(\mu\text{-dppm})(\mu\text{-}PhC{=}CH_2)(\mu\text{-}PPh_2)$] α-**I** and [$Fe_2(CO)_4(\mu\text{-dppm})(\mu\text{-}HC{=}CHPh)(\mu\text{-}PPh_2)$] β-**I** and found

Table 1 Selected bond lengths (Å) and angles (°) for complexes **1a**, **1c**, **2a**, **3a**, **6** and **7**

						7		
	1a	**1c**	**2a**	**3a**	**6**	Molecule A	Molecule B	Molecule C
Fe_σ–C_α	2.007(5)	2.027(11)	1.996(4)	1.955(4)	1.996(5)	1.972(10)	1.984(10)	1.981(10)
Fe–Fe	2.6153(12)	2.629(2)	2.6166(11)	2.6427(8)	2.6367(11)	2.641(2)	2.633(2)	2.611(2)
Fe_π–C_α	2.109(5)	2.126(12)	2.119(4)	2.079(4)	2.121(5)	2.093(11)	2.110(9)	2.087(11)
Fe_π–C_β	2.165(6)	2.188(11)	2.269(3)	2.228(4)	2.261(5)	2.235(11)	2.225(9)	2.211(11)
C_α–C_β	1.393(8)	1.402(14)	1.405(5)	1.405(5)	1.417(8)	1.40(2)	1.405(13)	1.397(14)
Fe_σ–PPh_2	2.229(2)	2.260(3)	2.2508(12)	2.2054(11)	2.246(2)	2.214(3)	2.206(3)	2.224(3)
Fe_π–PPh_2	2.252(2)	2.295(3)	2.2940(11)	2.2524(12)	2.295(2)	2.270(3)	2.279(3)	2.270(3)
Fe_σ–PR_3				2.2558(11)	2.230(2)	2.184(3)	2.183(3)	2.186(3)
Fe_π–PR_3						2.168(4)	2.177(3)	2.166(3)
Fe–PPh_2–Fe	71.43(5)	70.49(9)	70.29(4)	72.71(4)	70.98(5)	72.15(10)	71.89(10)	71.03(10)
Fe–C_α–Fe	78.8(2)	78.5(4)	78.91(13)	81.79(14)	79.6(2)	81.0(4)	80.0(3)	79.8(4)
Fe_σ–C_α–C_β	121.3(4)	124.4(8)	128.9(3)	128.5(3)	130.5(4)	132.6(9)	133.4(8)	129.8(8)
C_α–C_β–Fe_π	68.8(3)	68.6(6)	65.6(2)	65.3(2)	65.9(3)	65.7(6)	66.7(5)	66.3(6)
ΔC_α	0.102	0.099	0.123	0.124	0.125	0.121	0.126	0.106
ΔFe_π	0.056	0.062	0.150	0.149	0.140	0.142	0.115	0.124

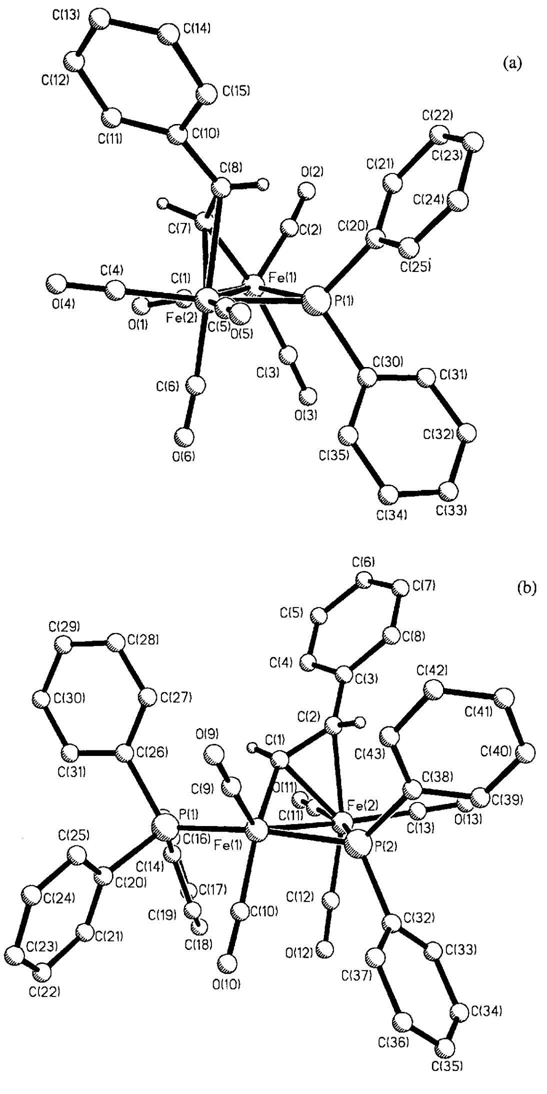

Fig. 2 Molecular structures of (a) complex **2a** and (b) **3a**.

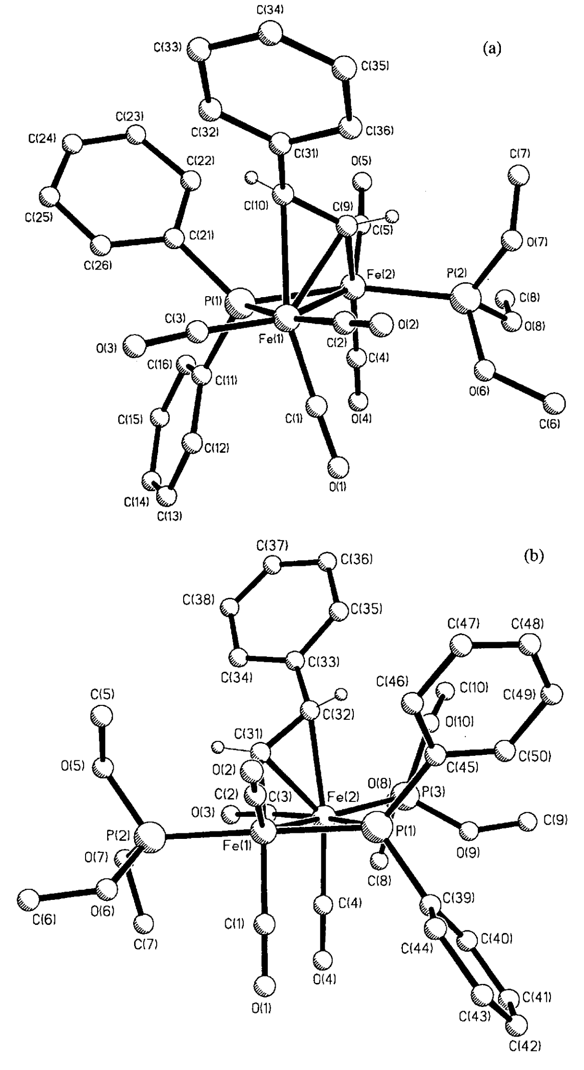

Fig. 3 Molecular structures of (a) complex **6** and (b) **7** (Molecule A).

significant structural differences.[9,13] Structural characterisation of **1a** and **2a** provides another isomeric pair for comparison, while a third set of phenylethenyl isomers, thiolate-bridged $[Fe_2(CO)_6(\mu\text{-}PhC{=}CH_2)(\mu\text{-}SBu^t)]$[25] α-**II** and $[Fe_2(CO)_6(\mu\text{-}HC{=}CHPh)(\mu\text{-}SBu^t)]$[28] β-**II** have also been characterised crystallographically. Table 2 gives a comparison of some key structural data for diiron alkenyl complexes and allows a comparison of isomeric pairs. In α-**I** and β-**I**, binding of the alkenyl ligand to the π-bound iron centre (Fe_π) varies greatly. For α-**I** it is bound almost symmetrically to both C_α and C_β (ΔFe_π – 0.015 Å), while in β-**I** the α-carbon lies closer by some 0.180 Å. The trend in ΔFe_π is consistent across all three isomeric pairs; that is, β isomers are more asymmetrically bound. This is especially apparent in the dppm-bridged complexes **I** where $\Delta\Delta Fe_\pi$ is 0.195 Å as compared to 0.094 Å between **1a**/**2a** and 0.135 Å in

Table 2 Selected bond lengths (Å) for diiron alkenyl complexes (esds omitted for clarity)

Complex	C_α–C_β	Fe_σ–C_α	Fe_σ–C_α	Fe_π–C_β	ΔC_α	ΔFe_π	Ref.
$[Fe_2(CO)_6(\mu\text{-}PhC{=}CHPh)(\mu\text{-}COEt)]$	1.423	2.011	2.059	2.185	0.048	0.126	4(*a*)
$[Fe_2(CO)_6(\mu\text{-}PhC{=}CHPh)(\mu\text{-}PPh_2)]$	1.424	2.039	2.099	2.223	0.060	0.124	29
$[Fe_2(CO)_6(\mu\text{-}PhC{=}CHPh)(\mu\text{-}AuPPh_3)]$	1.412	2.000	2.114	2.254	0.114	0.140	30
$[Fe_2(CO)_6(\mu\text{-}PhC{=}CHPh)(\mu\text{-}CH_2Ph)]$	1.440	2.000	2.088	2.201	0.088	0.113	31
$[Fe_2(CO)_4(\mu\text{-}dppm)(\mu\text{-}HC{=}CH_2)(\mu\text{-}PCy_2)]$	1.400	1.959	2.091	2.159	0.132	0.068	10
$[Fe_2(CO)_6(\mu\text{-}HC{=}CH_2)(\mu\text{-}SPh)]$	1.366	1.966	2.075	2.181	0.109	0.094	32
$]Fe_2(CO)_6(\mu\text{-}HC{=}CH_2)(\mu\text{-}PPh_2)]$	1.379	1.965	2.084	2.170	0.119	0.086	11
$[Fe_2(CO)_6(\mu\text{-}PhC{=}CH_2)(\mu\text{-}PPh_2)]$	1.393	2.007	2.109	2.165	0.102	0.056	This work
$[Fe_2(CO)_6(\mu\text{-}HC{=}CHPh)(\mu\text{-}PPh_2)]$	1.405	1.996	2.119	2.269	0.123	0.150	This work
$[Fe_2(CO)_4(\mu\text{-}dppm)(\mu\text{-}PhC{=}CH_2)(\mu\text{-}PPh_2)]$	1.416	1.998	2.156	2.141	0.158	−0.015	9
$[Fe_2(CO)_4(\mu\text{-}dppm)(\mu\text{-}HC{=}CHPh)(\mu\text{-}PPh_2)]$	1.397	1.979	2.106	2.286	0.127	0.180	13
$[Fe_2(CO)_6(\mu\text{-}PhC{=}CH_2)(\mu\text{-}SBu^t)]$	1.392	2.004	2.088	2.158	0.084	0.070	25
$[Fe_2(CO)_6(\mu\text{-}HC{=}CHPh)(\mu\text{-}SBu^t)]$	1.437	2.009	2.074	2.279	0.065	0.205	33
$[Fe_2(CO)_6(\mu\text{-}HC{=}CHPh)(\mu\text{-}Cl)]$	1.424	1.990	2.129	2.201	0.139	0.072	34
$[Fe_2(CO)_6(\mu\text{-}HC{=}CHPh)(\mu\text{-}SEt)]$	1.359	1.951	2.075	2.249	0.124	0.174	35
$[Fe_2(CO)_6(\mu\text{-}HC{=}CHPh)(\mu\text{-}SePh)]$	1.410	1.979	2.130	2.241	0.151	0.111	36
$[Fe_2(CO)_4(\mu\text{-}dppm)(\mu\text{-}HC{=}CHPh)(\mu\text{-}PCy_2)]$	1.394	1.972	2.104	2.262	0.132	0.158	10

thiolate-bridged **II**. Clearly, the *trans* influence of the dppm ligand plays a part in amplifying the effect. Similar values of ΔFe_π are seen for the other β-substituted isomers (**3a**, 0.149; **6**, 0.140; **7**, 0.115–0.142 Å), while α-substituted **1c** is far more symmetrically bound (ΔFe_π 0.062 Å). Thus, the origin of the larger values of ΔFe_π for β *vs.* α isomers is the elongation of the Fe_π–C_β bond and it is this which differentiates α and β isomers.

As the differences discussed above are based on a small sample size we have also examined a range of related crystallographically characterised diiron μ-alkenyl complexes (Table 2). Phenyl substitution at the α-carbon has little effect on the Fe_π–C_β bond. Thus, values of 2.159–2.181 Å (ΔFe_π 0.068–0.113 Å) in the unsubstituted alkenyl complexes can be compared with those of 2.141–2.165 Å (ΔFe_π −0.015 to 0.070 Å). In contrast, substitution at the β-carbon results in significant elongation to 2.201–2.286 Å (ΔFe_π 0.072–0.205 Å) and this is maintained in complexes with phenyl substituents on both α- and β-carbons (2.185–2.254 Å). From this structural data it is clear that there are significant differences between phenyl-substituted alkenyl complexes. Unfortunately, the lack of crystallographic data for alkyl substituted diiron μ-alkenyl complexes does not allow us to extend this conclusion.

While the structural studies clearly show that there are significant differences in the binding of the α- and β-substituted alkenyl moieties to the diiron centre, why this should lead to enhanced thermodynamic stability is still unclear. Carty and co-workers[11] have also distinguished α- and β-substituted diiron alkenyl complexes on the basis of ^{13}C NMR chemical shifts. Thus, for α-alkenyl complexes, C_α is shifted downfield (*δ* 178–220) with respect to its position for α-substituted or ethenyl complexes (*δ* 145–164), while C_β is shifted upfield (α, *δ* 48–75; β, *δ* 72–94). Specifically, **1a** (**2a**) are characterised by chemical shifts of *δ* 189.0 (145.7) and 66.2 (95.6) for C_α and C_β respectively. These data suggest that α-substituted complexes have a greater contribution from a metallacyclic resonance structure (**B**) than the metallaolefin formulation (**A**), and this

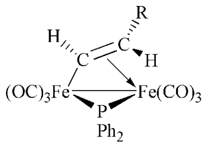

(A)
metallaolefin
β-isomers

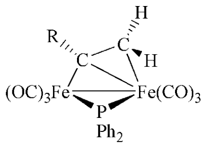

(B)
metallacyclic
α-isomers

imparts a degree of sp^3-like character to C_β. This view concurs with the structural data, in that as the β-carbon develops more sp^3 character then the Fe_π–C_β bond length is expected to decrease. Hence it appears that it is the decrease in metallacycle character seen in β isomers which leads to their greater thermodynamic stability.

Conclusion

This work has shown unequivocally for the first time that α–β alkenyl isomerisation can occur at the binuclear centre. Kinetically stable α-alkenyl complexes $[Fe_2(CO)_6(\mu\text{-}RC{=}CH_2)(\mu\text{-}PPh_2)]$ **1**, resulting from regioselective hydrodimetallation of primary alkynes, rearrange to the thermodynamically stable β isomers $[Fe_2(CO)_6(\mu\text{-}HC{=}CHR)(\mu\text{-}PPh_2)]$ **2** upon heating. Isomerisation is believed to occur *via* oxidative addition of a β-proton to the diiron centre and is accelerated in the presence of phosphines and phosphites. Detection of the intermediate phosphine-substituted α-alkenyl complex $[Fe_2(CO)_5(PPh_3)(\mu\text{-}MeC{=}CH_2)(\mu\text{-}PPh_2)]$ **3j′** by NMR and isolation of $[Fe_2(CO)_5\{P(OMe)_3\}(\mu\text{-}PhC{=}CH_2)(\mu\text{-}PPh_2)]$ **4** and $[Fe_2(CO)_4\{P(OMe)_3\}_2(\mu\text{-}PhC{=}CH_2)(\mu\text{-}PPh_2)]$ **5** show that carbonyl substitution precedes alkenyl isomerisation and it is the former which is rate-limiting. Acceleration of α–β alkenyl isomerisation upon substitution may result from an increase in electron density at the metal centre, making oxidative addition more favourable. However, steric effects cannot be ruled out and carbonyl substitution in α-alkenyl complexes may lead to adverse steric interactions between the alkenyl ligand, the phosphido-bridge and the incoming ligand which are relieved upon isomerisation.

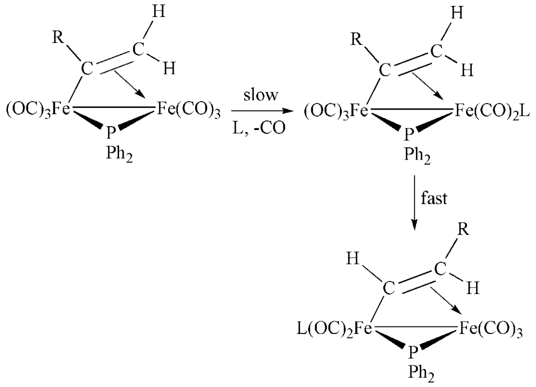

In earlier work we have described the reactivity of $[Fe_2(CO)_6(\mu\text{-}PhC{=}CH_2)(\mu\text{-}PPh_2)]$ **1a** towards the bidentate phosphines dppm[12] and dppe.[14] For both, phosphine substitution and CO insertion into the alkenyl ligand occur at 90 °C giving bridging α–β unsaturated acyl complexes $[Fe_2(CO)_4\{\mu\text{-}O{=}CC(Ph){=}CH_2\}(\mu\text{-}PPh_2)(\mu\text{-}dppm)]$ and $[Fe_2(CO)_n\{\mu\text{-}O{=}CC(Ph){=}CH_2\}(\mu\text{-}PPh_2)(dppe)]$ ($n = 3$ or 4) respectively. The key feature of these experiments is that phosphine substitution has occurred *without* α–β alkenyl isomerisation. Clearly, carbonyl insertion into the alkenyl ligand becomes favourable with respect to alkenyl isomerisation. Interestingly, however, prolonged thermolysis of [Fe$_2$(CO)$_4${μ-O=CC(Ph)=CH$_2$}(μ-PPh$_2$)(μ-dppm)] results in both carbonyl loss and α–β alkenyl isomerisation giving [Fe$_2$(CO)$_4$(μ-HC=CHPh)(μ-PPh$_2$)(μ-dppm)] in high yield.[12] This provides further evidence that alkenyl isomerisation proceeds *via* oxidative addition of a proton to a terminal site on the metal centre as the two bridging sites *cis* to the alkenyl ligand are blocked by the phosphido and diphosphine ligands.

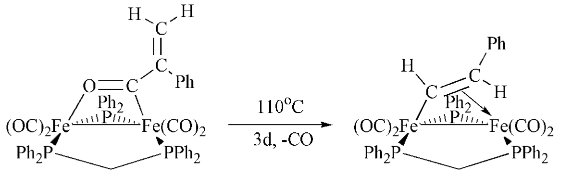

α–β Alkenyl isomerisation in diiron phosphido-bridged complexes may be more common than previously thought. Thus we note that, while a large number of α-substituted diiron hexacarbonyl alkenyl complexes are known, phosphine substituted derivatives remain elusive. This suggests that alkenyl isomerisation and its acceleration by phosphines may be a common trait in this area of chemistry. Fässler and Huttner[25] have reported the synthesis of thiolate-bridged trimethyl phosphite complexes [Fe$_2$(CO)$_5${P(OMe)$_3$}(μ-PhC=CH$_2$)(μ-SBu^t)] and [Fe$_2$(CO)$_4${P(OMe)$_3$}$_2$(μ-PhC=CH$_2$)(μ-SBu^t)], analogues of **4** and **5** respectively, at 60 °C, and it remains to be seen whether they undergo facile alkenyl isomerisation. Indeed, given the previous results of Knox and co-workers,[7,8] α–β alkenyl isomerisation at a binuclear centre may be widespread.

Experimental

General

All reactions were carried out under nitrogen using standard vacuum line techniques and dried and degassed solvents. Chromatography was carried out on deactivated alumina (6% w/w distilled water) wet packed with light petroleum (bp 40–60 °C) unless otherwise stated. The solution to be separated was added to alumina (3–5 g) and the solvent removed under reduced pressure. The resulting solids were then deposited on top of the prepared column and separation effected by elution with progressively more polar solvents. Alkynes and phosphines were purchased from Aldrich or Strem and used as supplied while Na[Fe$_2$(CO)$_{7/8}$(μ-PPh$_2$)]·1.5THF[37] was prepared *via* the literature method.

The IR spectra were recorded on a Nicolet 205 FTIR spectrometer, NMR spectra on Varian VXR-400, Bruker AMX400 and Avance500 spectrometers internally referenced to residual solvent peaks (^{1}H, ^{13}C) or externally to P(OMe)$_3$ (^{31}P), mass spectra on VG 7070 high resolution and VG Analytical ZAB2F spectrometers. Elemental analyses were performed in house.

Syntheses

[Fe$_2$(CO)$_6$(μ-RC=CH$_2$)(μ-PPh$_2$)] 1. A dichloromethane solution (20 cm^3) of Na[Fe$_2$(CO)$_{7/8}$(μ-PPh$_2$)]·1.5THF (0.55 g, 0.83 mmol) was cooled to −78 °C and HBF$_4$·Et$_2$O (0.15 cm^3) added dropwise by syringe. The resulting solution was stirred for 20 min and then allowed to warm slowly to room temperature. To this was added a slight excess of alkyne (*ca.* 0.1 cm^3) and stirring at room temperature for 16 h resulted in the formation of a bright orange solution. Volatiles were removed under reduced pressure and chromatography gave a yellow-orange band eluting with light petroleum (bp 40–60 °C) which afforded complexes **1a**–**1e**.

1a (R = Ph) (80% yield): ν(CO)(C$_6$H$_{14}$) 2060m, 2028s, 1994m, 1980m and 1964w cm^{-1}; ^{1}H NMR (CDCl$_3$) δ 7.8–6.7 (m, 15H, Ph), 3.12 (dd, *J* 14.8, 2.8, 1H, H$_\beta$) and 2.33 (dd, *J* 10.4, 2.8 Hz, 1H, H$_\beta$); ^{31}P NMR (CDCl$_3$) δ 180.3 (s, μ-PPh$_2$).

1b (R = Me) (34% yield): ν(CO)(C$_6$H$_{14}$) 2061m, 2026s, 1992m, 1980m and 1969w cm^{-1}; ^{1}H NMR (CDCl$_3$) δ 7.5–7.0 (m, 10H, Ph), 2.91 (dd, *J* 15.2, 2.2, 1H, H$_\beta$), 2.76 (s, 3H, CH$_3$) and 2.13 (dd, *J* 9.9, 2.2 Hz, 1H, H$_\beta$); ^{31}P NMR (CDCl$_3$) δ 179.5 (s, μ-PPh$_2$).

1c (R = Pr^n) (62% yield): ν(CO)(C$_6$H$_{14}$) 2062m, 2026s, 1991s, 1979s, 1965m and 1953w cm^{-1}; ^{1}H NMR (CDCl$_3$) δ 7.6–7.0 (m, 10H, Ph), 3.31 (m, 1H, CH$_2$), 2.89 (d, *J* 15.3, 1H, H$_\beta$), 2.08 (d, *J* 9.8, 1H, H$_\beta$), 2.07 (m, 1H, CH$_2$), 1.90 (m, 1H, CH$_2$), 1.61 (m, 1H, CH$_2$) and 0.96 (t, *J* 7.1 Hz, 3H, CH$_3$); ^{31}P NMR (CDCl$_3$) δ 180.0 (s, μ-PPh$_2$); mass spectrum (FAB) *m*/*z* 534 (M$^+$), 506, 478, 450, 422, 394 and 366 (M$^+$ − 6CO); calc. for C$_{23}$H$_{19}$Fe$_2$O$_6$P C 51.68, H 3.54; found C 51.83, H 3.32%.

1d (R = Bu^n) (34% yield): ν(CO)(C$_6$H$_{14}$) 2062m, 2025vs, 1991s, 1979s, 1965s and 1954m cm^{-1}; ^{1}H NMR (CDCl$_3$) δ 7.8–7.2 (m, 10H, Ph), 3.45 (dt, *J* 15.0, 4.3, 1H, C^{2}H$_2$), 3.04 (dd, *J* 15.3, 2.5, 1H, H$_\beta$), 2.27 (m, 1H, C^{2}H$_2$), 2.12 (dd, *J* 12.9, 4.3, 1H, H$_\beta$), 1.97 (m, 1H, C^{4}H$_2$), 1.74 (m, 1H, C^{4}H$_2$), 1.57 (m, 1H, C^{3}H$_2$), 1.48 (m, 1H, C^{3}H$_2$) and 1.03 (t, *J* 7.3 Hz, 3H, CH$_3$); ^{31}P NMR (CDCl$_3$) δ 180.0 (s, μ-PPh$_2$); ^{13}C NMR (CDCl$_3$) δ 212.5 (s, 4CO), 211.63 (d, *J* 21.7, CO), 211.57 (d, *J* 20.1, CO), 192.5 (d, *J* 19.8, C$_\alpha$), 139.0 (d, *J* 44.1, C$_{ipso}$), 135.4 (d, *J* 28.0, C$_{ipso}$), 133.8 (d, *J* 6.4, Ph), 133.4 (d, *J* 7.4, Ph), 132.3 (s, Ph), 130.5 (d, *J* 12.5, Ph), 130.1 (s, Ph), 130.0 (s, Ph), 128.7 (d, *J* 11.0, Ph), 128.3 (d, *J* 9.8, Ph), 70.1 (d, *J* 13.6 Hz, C$_\beta$), 60.0 (s, CH$_2$), 38.5 (s, CH$_2$), 22.6 (s, CH$_2$) and 14.0 (s, CH$_3$).

1e (R = Bu^t) (70% yield): ν(CO)(C$_6$H$_{14}$) 2053m, 2019vs, 1982s, 1974s, 1965m and 1954w cm^{-1}; ^{1}H NMR (CDCl$_3$) δ 7.8–7.2 (m, 10H, Ph), 3.38 (dd, *J* 16.2, 4.4, 1H, H$_\beta$), 2.06 (dd, *J* 13.1, 4.4 Hz, 1H, H$_\beta$) and 1.46 (s, 9H, CH$_3$); ^{31}P NMR (CDCl$_3$) δ 179.9 (s, μ-PPh$_2$).

[Fe$_2$(CO)$_6$(μ-PhC=CHMe)(μ-PPh$_2$)] **1f** (85% yield): ν(CO)(C$_6$H$_{14}$) 2058s, 2022vs, 1990s, 1980s and 1966m cm^{-1}; ^{1}H NMR (CDCl$_3$) δ 7.8–7.2 (m, 15H, Ph), 3.15 (dq, *J* 12.1, 6.0, 1H, H$_\beta$) and 1.28 (d, *J* 6.0 Hz, 3H, Me); ^{13}C NMR (CDCl$_3$) δ 216–218 (br, CO), 184.8 (d, *J* 20.4, C$_\alpha$), 153.1 (s, C$_{ipso}$), 138.7 (d, *J* 46.1, C$_{ipso}$), 134.7 (d, *J* 30.4, C$_{ipso}$), 134–126 (m, Ph), 80.7 (d, *J* 15.6, C$_\beta$) and 23.1 (d, *J* 5.1 Hz, Me); ^{31}P NMR (CDCl$_3$) 173.3 (s, μ-PPh$_2$); mass spectrum (FAB) *m*/*z* 554 (M − CO), 526 (M − 2CO), 498 (M − 3CO), 470 (M − 4CO), 442 (M − 5CO) and 414 (M − 6CO); calc. for C$_{27}$H$_{19}$Fe$_2$O$_6$P C 55.67, H 3.26; found, C 55.77, H 3.26%.

[Fe$_2$(CO)$_6$(μ-HC=CHR)(μ-PPh$_2$)] 2. Thermolysis of a toluene solution (15 cm^3) of complex **1** (70 mg) for between 45 min and 4 h resulted in a slight lightening of the solution. After removal of volatiles chromatography gave a yellow band eluting with light petroleum which yielded **2a**–**2e**.

2a (R = Ph) (95% yield after 1 h): ν(CO)(C$_6$H$_{14}$) 2064m, 2029sm, 1999m and 1984m and 1971w cm^{-1}; ^{1}H NMR (CDCl$_3$) δ 8.85 (dd, *J* 13.5, 6.2, 1H, H$_\alpha$), 7.8–7.1 (m, 13H, Ph), 6.87 (d, *J* 7.0, 2H, Ph) and 4.06 (dd, *J* 13.5, 5.0 Hz, 1H, H$_\beta$); ^{31}P NMR (CDCl$_3$) δ 180.3 (s, μ-PPh$_2$).

2b (R = Me) (45% yield after 4 h): ν(CO)(C$_6$H$_{14}$) 2064m, 2026s, 1997m, 1982m and 1969w cm^{-1}; ^{1}H NMR (CDCl$_3$) δ 7.96 (dd, *J* 12.4, 6.2, 1H, H$_\alpha$), 7.6–7.1 (m, 10H, Ph), 3.21 (dq, *J* 6.2, 5.4, 1H, H$_\beta$) and 1.52 (d, *J* 5.4 Hz, 3H, CH$_3$); ^{31}P NMR (CDCl$_3$) δ 181.1 (s, μ-PPh$_2$).

2c (R = Pr^n) (28% yield after 3 h): ν(CO)(C$_6$H$_{14}$) 2063s, 2026vs, 1996s, 1981s, 1965s and 1953m cm^{-1}; ^{1}H NMR (CDCl$_3$) δ 7.9 (br, 1H, H$_\alpha$), 7.6–7.0 (m, 10H, Ph), 3.28 (br, 1H, H$_\beta$), 1.76 (br, 2H, CH$_2$), 1.31 (br, 2H, CH$_2$) and 0.71 (br, 3H, CH$_3$); ^{31}P NMR (CDCl$_3$) δ 180.9 (s, μ-PPh$_2$).

2d (R = Bu^n) (38% yield after 45 min): ν(CO)(C_6H_{14}) 2063s, 2026s, 1995s, 1981m, 1965s and 1954m cm^{-1}; ^{1}H NMR ($CDCl_3$) δ 7.95 (dd, *J* 12.7, 5.9, 1H, H_α), 7.8–7.2 (m, 10H, Ph), 3.16 (m, 1H, H_β), 1.65 (m, 2H, CH_2), 1.16 (m, 2H, CH_2), 0.83 (m, 2H, CH_2) and 0.71 (t, *J* 7.2 Hz, 3H, CH_3); ^{31}P NMR ($CDCl_3$) δ 180.8 (s, μ-PPh_2).

2e (R = Bu^t) (70% yield after 45 min): ν(CO)(C_6H_{14}) 2062s, 2024s, 1995s, 1980s, 1966m and 1953m cm^{-1}; ^{1}H NMR ($CDCl_3$) δ 7.91 (dd, *J* 14.0, 5.6, 1H, H_α), 7.8–7.2 (m, 10H, Ph), 3.39 (dd, *J* 14.0, 5.2 Hz, 1H, H_β) and 0.82 (s, 9H, Bu^t); ^{31}P NMR ($CDCl_3$) δ 180.0 (s, μ-PPh_2).

[$Fe_2(CO)_6$(μ-HC=CHCH$_2$Ph)(μ-PPh_2)] **2f**. Thermolysis of a toluene solution (15 cm^3) of complex **1f** (60 mg) for 1 h resulted in consumption of starting material as shown by IR spectroscopy. After removal of volatiles chromatography gave a yellow band eluting with light petroleum which yielded **2f** (42%). ν(CO)(C_6H_{14}) 2063s, 2028s, 1997s, 1988m, 1982s and 1970w cm^{-1}; ^{1}H NMR ($CDCl_3$) δ 8.10 (dd, *J* 12.4, 6.5, 1H, H_α), 7.53 (m, 2H, Ph), 7.4–7.2 (m, 11H, Ph), 6.74 (d, *J* 2.6, 1H, Ph), 6.73 (s, 1H, Ph), 3.34 (quintet, *J* 6.5 Hz, 1H, H_β) and 3.03 (br, 2H, CH_2); (233 K) δ 8.11 (dd, *J* 12.3, 6.2, 1H, H_α), 7.53 (m, 2H, Ph), 7.45–7.15 (m, 11H, Ph), 6.68 (m, 2H, Ph), 3.35 (dd, *J* 14.0, 7.3, 1H, CH_2), 3.29 (quintet, *J* 6.8, 1H, H_β) and 2.66 (dd, *J* 14.0, 7.0 Hz, 1H, CH_2); ^{31}P NMR ($CDCl_3$) 180.8 (s, μ-PPh_2); mass spectrum (FAB) *m*/*z* 582 (M$^+$), 554 (M − CO), 526 (M − 2CO), 498 (M − 3CO), 470 (M − 4CO), 442 (M − 5CO) and 414 (M − 6CO).

[$Fe_2(CO)_5$(PR′$_3$)(μ-HC=CHR)(μ-PPh_2)] 3. A toluene solution (20 cm^3) of complex **1a** (80 mg, 0.14 mmol) and PPh_3 (0.040 g, 0.15 mmol) was heated to reflux for 10 minutes, during which time a change from orange to red occurred. After cooling to room temperature, chromatography on alumina gave a red band with diethyl ether–light petroleum (2 : 3) which afforded **3a** as a dry red solid. Recrystallisation from a dichloromethane–methanol mixture gave thin orange plates suitable for X-ray crystallography. All other complexes were prepared in an analogous fashion.

3a (R = Ph, R′ = Ph) (95% yield after 10 min): ν(CO) (CH_2Cl_2) 2034m, 1983vs, 1947s, 1917m and 1884w cm^{-1}; ^{1}H NMR ($CDCl_3$) δ 8.35 (ddd, *J* 27.9, 12.9, 6.5, 1H, H_α), 7.9–6.4 (m, 30H, Ph) and 4.12 (dd, *J* 12.9, 5.4 Hz, 1H, H_β); ^{31}P NMR ($CDCl_3$) δ 181.2 (d, *J* 93.4, μ-PPh_2) and 73.0 (d, *J* 93.4 Hz, PPh_3); ^{13}C NMR ($CDCl_3$) 218.9 (t, *J* 14.5, CO), 214.5 (br, 2CO), 212.7 (dd, *J* 21.5, 17.5, CO), 209.8 (br, CO), 153.6 (t, *J* 24.7, C_α), 142.2 (s, C_{ipso}), 140.5 (d, *J* 42.6, C_{ipso}), 137.3 (d, *J* 19.8, C_{ipso}), 134.6 (s), 134.0 (d, *J* 9.2), 133.6 (s), 130.1 (s), 129.5 (d, *J* 25.0), 128.4 (d, *J* 8.6), 128.2 (d, *J* 19.4), 126.0 (s), 125.0 (s) and 89.4 (d, *J* 15.2 Hz, C_β); mass spectrum (FAB) *m*/*z* 802 (M$^+$), 746 (M − 2CO), 718 (M − 3CO), 690 (M − 4CO) and 662 (M − 5CO); calc. for $C_{43}H_{32}Fe_2O_5P_2$ C 64.34, H 3.99; found C 65.02, H 4.67%.

3b (R = Ph, R′ = *p*-tolyl) (71% yield after 10 min): ν(CO) (CH_2Cl_2) 2030m, 1982vs, 1946s, 1917m and 1885w cm^{-1}; ^{1}H NMR ($CDCl_3$) δ 8.35 (ddd, *J* 27.8, 12.9, 6.5, 1H, H_α), 7.8–7.0 (m, 25H, Ph), 6.62 (d, *J* 7.5, 2H, Ph), 4.13 (dd, *J* 12.9, 5.3 Hz, 1H, H_β) and 2.36 (s, 9H, Me); ^{31}P NMR ($CDCl_3$) δ 180.6 (d, *J* 93.9, μ-PPh_2) and 72.0 (d, *J* 93.9, PAr$_3$); ^{13}C NMR ($CDCl_3$) δ 219.1 (t, *J* 15.6, CO), 214.6 (br, 2CO), 212.9 (t, *J* 21.3, CO), 210 (vbr, CO), 154.1 (t, *J* 26.2, C_α), 142.3 (s, C_{ipso}), 140.3 (d, *J* 33.0, C_{ipso}), 140.1 (s), 137.4 (d, *J* 20.7, C_{ipso}), 133.9 (d, *J* 10.0), 133.5 (s), 131.3 (d, *J* 40.6), 129.5 (s), 129.1 (d, *J* 9.5), 128.8 (s), 128.1 (d, *J* 22.9), 125.8 (s), 125.0 (s), 89.3 (d, *J* 17.1 Hz, C_β) and 21.3 (s, CH_3); mass spectrum (FAB) *m*/*z* 844 (M$^+$), 788 (M − 2CO), 760 (M − 3CO), 732 (M − 4CO) and 704 (M − 5CO); calc. for $C_{46}H_{38}Fe_2O_5P_2$ C 65.40, H 4.50; found, C 65.64, H 4.83%.

3c (R = Ph, R′ = *m*-tolyl) (93% yield after 10 min): ν(CO) (CH_2Cl_2) 2033m, 1982vs, 1970sh, 1949m and 1915m cm^{-1}; ^{1}H NMR ($CDCl_3$) δ 8.31 (ddd, *J* 27.8, 12.9, 6.5, 1H, H_α), 7.8–7.0 (m, 25H, Ph), 6.58 (d, *J* 7.1, 2H, Ph), 4.08 (dd, *J* 12.8, 5.4 Hz, 1H, H_β) and 2.37 (s, 9H, Me); ^{31}P NMR ($CDCl_3$) δ 180.6 (d, *J* 94.4, μ-PPh_2) and 70.6 (d, *J* 94.4 Hz, PAr$_3$); ^{13}C NMR ($CDCl_3$) δ 219.0 (t, *J* 15.4, CO), 214.8 (br, 2CO), 212.9 (dd, *J* 20.8, 17.2, CO), 210 (vbr, CO), 154.0 (t, *J* 24.6, C_α), 142.4 (s, C_{ipso}), 140.2 (d, *J* 42.1, C_{ipso}), 138.0 (d, *J* 9.1), 137.7 (d, *J* 9.8, C_{ipso}), 137.4 (d, *J* 8.5), 134.5 (s), 134.1 (s), 133.6 (d, *J* 5.8), 132.4 (s), 131.0 (d, *J* 25.9), 130.8 (s), 129.4 (d, *J* 18.3), 128.9 (s), 128.8 (s), 125.9 (d, *J* 21.4), 125.0 (s), 89.4 (d, *J* 15.3, C_β) and 21.6 (s, CH_3); mass spectrum (FAB) *m*/*z* 844 (M$^+$), 788 (M − 2CO), 760 (M − 3CO), 732 (M − 4CO) and 704 (M − 5CO); calc. for $C_{46}H_{38}Fe_2O_5P_2$ C 65.40, H 4.50; found C 65.22, H 4.49%.

3d (R = Ph, R′ = p-FC$_6$H$_4$) (62% yield after 10 min): ν(CO)(CH_2Cl_2) 2035s, 1985vs, 1952m and 1918m cm^{-1}; ^{1}H NMR ($CDCl_3$) δ 8.20 (ddd, *J* 34.8, 12.9, 6.3, 1H, H_α), 7.8–7.0 (m, 25H, Ph), 6.58 (d, *J* 6.9, 2H, Ph) and 4.11 (dd, *J* 13.0, 5.5 Hz, 1H, H_β); ^{31}P NMR ($CDCl_3$) δ 182.5 (d, *J* 95.8, μ-PPh_2) and 71.9 (d, *J* 95.8, PAr$_3$); ^{13}C NMR ($CDCl_3$) δ 218.5 (t, *J* 15.8, CO), 214.1 (br, 2CO), 212.5 (t, *J* 21.0, CO), 209.8 (br, CO), 163.9 (d, *J* 252.9, C_{ipso}F), 152.9 (t, *J* 24.6, C_α), 141.8 (s, C_{ipso}), 139.9 (d, *J* 42.7, C_{ipso}), 136.9 (d, *J* 23.2, C_{ipso}), 135.9 (d, *J* 18.9), 135.9 (s), 135.2 (d, *J* 5.2), 133.5 (s), 130.2 (s), 129.6 (d, *J* 25.9), 128.3 (d, *J* 27.8), 126.3 (s), 124.9 (s), 116.0 (dd, *J* 21.4, 10.5) and 89.9 (d, *J* 15.9 Hz, C_β); mass spectrum (FAB) *m*/*z* 856 (M$^+$), 800 (M − 2CO), 772 (M − 3CO), 744 (M − 4CO) and 716 (M − 5CO); calc. for $C_{43}H_{29}F_3Fe_2O_5P_2$ C 60.28, H 3.39; found C 59.84, H 3.35%.

3e (R = Ph, R′ = CH$_2$CH$_2$CN) (98% yield after 20 min): ν(CO)(CH_2Cl_2) 2036m, 1982vs, 1952m and 1922m cm^{-1}; ^{1}H NMR ($CDCl_3$) δ 8.08 (ddd, *J* 27.5, 12.8, 6.0, 1H, H_α), 7.7–7.1 (m, 13H, Ph), 6.80 (d, *J* 7.6, 2H, Ph), 4.03 (dd, *J* 12.8, 5.5, 1H, H_β), 2.87 (q, *J* 7.4, 6H, CH_2) and 2.50 (dquin, *J* 49.9, 7.4 Hz, PCH$_2$); ^{31}P NMR ($CDCl_3$) δ 176.2 (d, *J* 89.2, μ-PPh_2) and 56.6 (d, *J* 89.2 Hz, PR′$_3$); mass spectrum (FAB) *m*/*z* 705 (M − CO), 677 (M − 2CO), 649 (M − 3CO) and 593 (M − 5CO); calc. for $C_{34}H_{29}Fe_2N_3O_5P_2$ C 55.66, H 3.96, N 5.73; found, C 55.58, H 3.91, N 5.57%.

3f (R = Ph, R′ = Me) (65% yield after 10 min): ν(CO)-(CH_2Cl_2) 2026m, 1978vs, 1943s and 1918sh cm^{-1}; ^{1}H NMR ($CDCl_3$) δ 8.30 (br, 1H, H_α), 7.8–7.0 (m, 13H, Ph), 6.88 (d, *J* 6.7 Hz, 2H, Ph), 3.99 (br, 1H, H_β) and 1.64 (br, 9H, CH_3); ^{31}P NMR ($CDCl_3$) δ 175.2 (d, *J* 92.8, μ-PPh_2) and 27.3 (d, *J* 92.8 Hz, PMe$_3$); ^{13}C NMR ($CDCl_3$) δ 217.7 (br t, *J* 14, CO), 214.4 (br, 3CO), 212.1 (vbr, CO), 148.7 (br, C_α), 142.2 (s, C_{ipso}), 140.2 (d, *J* 42.5, C_{ipso}), 137.3 (d, *J* 21.0, C_{ipso}), 133.8 (s), 133.5 (d, *J* 6.1), 129.5 (d, *J* 36.6), 129.0 (s), 128.2 (s), 128.0 (s), 126.2 (s), 125.2 (s), 91.0 (br, C_β) and 18.2 (d, *J* 36.1 Hz, CH_3); mass spectrum (FAB) *m*/*z* 616 (M$^+$), 560 (M − 2CO), 532 (M − 3CO), 504 (M − 4CO) and 476 (M − 5CO).

3g (R = Ph, PR′$_3$ = PPh$_2$Me) (66% yield after 10 min): ν(CO)(CH_2Cl_2) 2030m, 1978vs, 1949m and 1916m cm^{-1}; ^{1}H NMR ($CDCl_3$) δ 8.12 (ddd, *J* 27.3, 12.9, 6.3, 1H, H_α), 7.8–6.9 (m, 23H, Ph), 6.52 (d, *J* 7.0, 2H, Ph), 3.99 (dd, *J* 12.9, 5.4, 1H, H_β) and 2.18 (d, *J* 7.5 Hz, 3H, CH_3); ^{31}P NMR ($CDCl_3$) δ 178.7 (d, *J* 92.5, μ-PPh_2) and 54.4 (d, *J* 92.5 Hz, PPh$_2$Me); mass spectrum (FAB) *m*/*z* 740 (M$^+$), 684 (M − 2CO), 656 (M − 3CO), 628 (M − 4CO) and 600 (M − 5CO).

3h (R = Ph, ER′$_3$ = AsPh$_3$) (14% yield after 1 h): ν(CO) (CH_2Cl_2) 2034m, 1981vs, 1952m and 1918m cm^{-1}; ^{1}H NMR ($CDCl_3$) δ 8.39 (dd, *J* 13.1, 4.7, 1H, H_α), 7.7–7.2 (m, 24H, Ph), 7.04–6.97 (m, 4H, Ph), 6.51 (d, *J* 7.9, 2H) and 4.06 (dd, *J* 13.2, 5.3 Hz, 1H, H_β); ^{31}P NMR ($CDCl_3$) δ 183.2 (s, μ-PPh_2); mass spectrum (FAB) *m*/*z* 846 (M$^+$), 790 (M − 2CO), 762 (M − 3CO), 734 (M − 4CO) and 706 (M − 5CO).

3i (R = Bu^t, R′ = Ph) (57% yield after 10 min): ν(CO) (CH_2Cl_2) 2030s, 1987vs, 1969s, 1951s and 1921s cm^{-1}; ^{1}H NMR ($CDCl_3$) δ 7.8–7.1 (m, 26H, Ph + H_α), 3.34 (dd, *J* 13.4, 5.8 Hz, 1H, H_β) and 0.70 (s, 9H, Bu^t); ^{31}P NMR ($CDCl_3$) δ 180.4 (d, *J* 93.9, μ-PPh_2) and 73.7 (d, *J* 93.9 Hz, PPh_3); mass spectrum (FAB) *m*/*z* 782 (M$^+$), 726 (M − 2CO), 670 (M − 4CO) and 642

(M − 5CO); calc. for $C_{41}H_{36}Fe_2O_5P_2$ C 62.91, H 4.60; found C 62.80, H 4.60%.

3j (R = Me, R′ = Ph) (93% yield after 1 h): *ν*(CO)(C_6H_{14}) 2034s, 1989vs, 1973s, 1955m and 1923m cm^{-1}; ^{1}H NMR ($CDCl_3$) *δ* 7.6–7.2 (m, 26H, Ph + H_α), 3.11 (sextet, *J* 5.7, 1H, H_β) and 1.34 (d, *J* 5.7 Hz, 3H, CH_3); ^{31}P NMR ($CDCl_3$) *δ* 177.3 (d, *J* 93.5, μ-PPh_2) and 67.6 (d, *J* 93.5 Hz, PPh_3); mass spectrum (FAB) *m*/*z* 740 (M^+), 684 (M − 2CO), 656 (M − 3CO), 628 (M − 4CO) and 600 (M − 5CO); calc. for $C_{38}H_{30}Fe_2O_5P_2\cdot0.75CH_2Cl_2$ C 57.85, H 3.92; found C 58.01, H 4.08%.

[$Fe_2(CO)_5(PPh_3)(\mu\text{-}MeC{=}CH_2)(\mu\text{-}PPh_2)$] 3j′. Heating complex **1b** and PPh_3 at 110 °C for 30 min gave an inseparable mixture of **1b**, **3j** and **3j′** (approximate ratio 1 : 2 : 2). ^{1}H NMR ($CDCl_3$) *δ* 7.6–7.1 (m, Ph), 2.29 (dd, *J* 7.9, 3.0, 1H, H_β), 2.19 (s, *J* 5.7, 3H, CH_3) and 2.07 (ddd, *J* 15.3, 6.7, 3.0, 1H, H_β): ^{31}P NMR ($CDCl_3$) *δ* 168.5 (d, *J* 63.4, μ-PPh_2) and 64.1 (d, *J* 63.4 Hz, PPh_3).

[$Fe_2(CO)_5\{P(OMe)_3\}(\mu\text{-}PhC{=}CH_2)(\mu\text{-}PPh_2)$] 4 and [$Fe_2(CO)_4\{P(OMe)_3\}_2(\mu\text{-}PhC{=}CH_2)(\mu\text{-}PPh_2)$] 5. A toluene solution (20 cm^3) of complex **1a** (0.110 g, 0.19 mmol) and $P(OMe)_3$ (50 mg, 0.40 mmol) was heated at 65 °C for 5 minutes, during which time a change from orange to red occurred. After cooling to room temperature, chromatography on alumina gave an orange band with diethyl ether–light petroleum (1 : 9) which afforded **4** (60 mg, 47%) as a dry orange solid, while further elution with diethyl ether–light petroluem (1 : 5) gave a second orange band which afforded **5** (50 mg, 34%) as a dry orange solid.

4 (two isomers A : B in 2 : 1 ratio at 213 K): *ν*(CO)(CH_2Cl_2) 2035s, 1987vs, 1971m and 1958s cm^{-1}; ^{1}H NMR ($CDCl_3$) *δ* 7.8–7.1 (m, Ph), 3.65 (d, *J* 11.2, Me, 9H, A), 3.60 (d, *J* 11.2, Me, 9H, B), 3.16 (d, *J* 15.2, 1H, B), 3.01 (dt, *J* 15.4, 3.3, 1H, A), 2.28 (dt, *J* 12.1, 3.3, 1H, A) and 2.24 (d, *J* 10.5 Hz, 1H, B); ^{31}P NMR ($CDCl_3$) (213 K) *δ* 188.1 (d, *J* 52.7, $P(OMe_3)$, B), 186.6 (d, *J* 70.2, $P(OMe_3)$, A), 165.0 (d, *J* 70.2, PPh_2, A) and 152.5 (d, *J* 52.7, PPh_2, B); (d^8-toluene) (383 K) *δ* 164 (br) and 181.8 (d, *J* 46.8 Hz); ^{13}C NMR ($CDCl_3$) 215.7 (t, *J* 14.6, 2CO, B), 215.5 (d, *J* 24.4, 2CO, B), 215.1 (s, 2CO, A), 213.2 (s, CO, B), 210.9 (s, 3CO, A), 189.5 (d, *J* 19.9, C_α, A), 188.9 (d, *J* 19.3, C_α, B), 158.6 (s, C_{ipso}, B), 156.1 (s, C_{ipso}, A), 141.1 (d, *J* 43.3, C_{ipso}, A), 140.6 (d, *J* 44.4, C_{ipso}, B), 136.2–125.4 (m), 66.8 (d, *J* 14.6, C_β, B), 62.6 (dd, *J* 12.0, 5.3 Hz, C_β, A) and 52.2 (m, OCH_3, A + B); calc. for $C_{28}H_{26}Fe_2O_8P_2$ C 50.60, H 3.92; found C 50.23, H 3.79%.

5: *ν*(CO)(CH_2Cl_2) 1997vs, 1962s and 1932m cm^{-1}; ^{1}H NMR ($CDCl_3$) *δ* 7.8–7.1 (m, 15H, Ph), 3.55 (d, *J* 11.2, 9H, Me), 3.51 (d, *J* 11.2, 9H, Me), 3.00 (d, *J* 16.1, 1H) and 2.15 (d, *J* 10.8 Hz, 1H); ^{31}P NMR ($CDCl_3$) (213 K) 189.8 (d, *J* 47.0, $P(OMe)_3$), 189.1 (d, *J* 71.6) and 145.9 (br, PPh_2); (d^8-toluene) (383 K) *δ* 160.4 (t, *J* 44.9) and 183.8 (br d); ^{13}C NMR ($CDCl_3$) (223 K) *δ* 218.0 (d, *J* 8.6, CO), 216.6 (t, *J* 24.4, CO), 214.3 (m, br, CO), 211.3 (br, CO), 185.3 (br d, *J* 10.3, C_α), 159.7 (s, C_{ipso}), 142.5 (d, *J* 43.0, C_{ipso}), 136.8 (d, *J* 21.6, C_{ipso}), 136.2 (s), 134.3 (s), 130.7 (s), 128.7 (s), 127.5(s), 126.4 (d, *J* 26.5 Hz), 125.8 (s), 62.4 (br s, C_β), 52.3 (s, OCH_3) and 52.0 (s, OCH_3); mass spectrum (FAB) *m*/*z* 760 (M^+), 704 (M − 2CO), 676 (M − 3CO) and 648 (M − 4CO); calc. for $C_{30}H_{35}Fe_2O_{10}P_2$ C 47.37, H 3.95; found C 47.35, H 4.59%.

[$Fe_2(CO)_5\{P(OMe)_3\}(\mu\text{-}HC{=}CHPh)(\mu\text{-}PPh_2)$] 6. A toluene solution (10 cm^3) of complex **4** (25 mg) was heated to reflux for 30 minutes, during which time the yellow solution darkened slightly. After cooling to room temperature, chromatography on alumina gave a yellow band with diethyl ether–light petroleum (1 : 10) which afforded **6** (23 mg, 92%) as a dry orange solid. Recrystallisation from a dichloromethane–ethanol mixture gave orange crystals suitable for X-ray crystallography. *ν*(CO) (CH_2Cl_2) 2037s, 1989vs, 1976s, 1956s and 1928m cm^{-1}: ^{1}H NMR ($CDCl_3$) (223 K) *δ* 8.73 (ddd, *J* 31.8, 12.7, 8.1, 1H, H_α), 7.8–6.8 (m, 15H, Ph), 3.79 (d, *J* 11.1, 9H, Me) and 3.73 (t, *J* 14.0, 1H, H_β); (d^8-toluene) (353 K) *δ* 8.91 (ddd, *J* 21.4, 13.4, 7.3, 1H, H_α), 7.68 (m, 4H, Ph), 7.0–6.7 (m, 11H, Ph), 4.21 (dd, *J* 13.4, 5.2, 1H, H_β) and 3.36 (d, *J* 10.9 Hz, 9H, Me) ^{31}P NMR ($CDCl_3$) (223 K) *δ* 182.6 (d, *J* 154.7, $P(OMe)_3$), 177.7 (d, *J* 154.7, PPh_2); (d^8-toluene) (353 K) *δ* 177.3 (d, *J* 125.9) and 172.4 (d, *J* 125.9 Hz). Mass spectrum (FAB): *m*/*z* 664 (M^+), 636 (M − CO), 608 (M − 2CO), 580 (M − 3CO), 552 (M − 4CO) and 524 (M − 5CO). Calc. for $C_{28}H_{26}Fe_2O_8P_2$ C 50.60, H 3.92; found, C 49.99, H 4.01%.

[$Fe_2(CO)_4\{P(OMe)_3\}_2(\mu\text{-}HC{=}CHPh)(\mu\text{-}PPh_2)$] 7. A toluene solution (10 cm^3) of complex **5** (25 mg) was heated to reflux for 30 minutes, during which time the yellow solution darkened slightly. After cooling to room temperature, chromatography on alumina gave a yellow band with diethyl ether–light petroleum (1 : 5) which afforded **7** (23 mg, 92%) as a dry orange solid. Recrystallisation from a dichloromethane–ethanol mixture gave orange crystals suitable for X-ray crystallography. Two isomers A : B in 6 : 1 ratio at 223 K: *ν*(CO)(CH_2Cl_2) 1995s, 1963vs, 1930s and 1910m cm^{-1}. ^{1}H NMR ($CDCl_3$) (223 K) *δ* 8.74 (ddd, *J* 30.2, 13.0, 8.1, 1H, H_α, A), 8.63 (br, 1H, H_α, B), 7.85–6.8 (m, 15H, Ph), 3.96 (br, 1H, H_β, B), 3.79 (d, *J* 11.2, 9H, Me, A), 3.73 (d, *J* 11.2, 9H, Me, B), 3.50 (d, *J* 11.5, 1H, H_β, A), 3.32 (d, *J* 11.0, 9H, Me, A) and 3.28 (br, 9H, Me, B); (d^8-toluene) (353 K) *δ* 8.99 (dddd, *J* 24.9, 13.6, 11.5, 2.1, H_α), 7.87 (t, *J* 10.1, 2H, Ph), 7.63 (m, 2H, Ph), 7.07–6.61 (m, 11H, Ph), 4.01 (dd, *J* 13.5, 4.7, 1H, H_β) and 3.34 (d, *J* 10.9 Hz, 18H, Me). ^{31}P NMR: ($CDCl_3$) (223 K) *δ* 196.8 (d, *J* 45.5, μ-$P(OMe)_3$, B), 188.6 (d, *J* 145.7, $P(OMe)_3$, A), 181.0 (d, *J* 150.7, $P(OMe)_3$, B), 180.3 (d, *J* 59.8 $P(OMe)_3$, A), 165.4 (dd, *J* 145.7, 59.8, PPh_2, A) and 159.0 (dd, *J* 150.7, 45.0, PPh_2, B); (d^8-toluene) (353 K) *δ* 180.9 (d, *J* 45.1) and 160.6 (t, *J* 45.1 Hz).

X-Ray data collection and solution

For complexes **1a**, **1c**, **2a**, **6** and **7** single crystals were mounted on glass fibres and all geometric and intensity data taken using an automated four-circle diffractometer (Nicolet R3mV) equipped with Mo-Kα radiation ($\lambda = 0.710\ 73$ Å) at 293 ± 2 K. The lattice parameters were identified by application of the automatic indexing routine of the diffractometer to the positions of a number of reflections taken from a rotation photograph and centred by the diffractometer. The *ω*–2*θ* or *ω* technique was used to measure reflections and three standard reflections (remeasured every 97 scans) showed no significant loss in intensity during data collection. The data were corrected for Lorentz and polarisation effects and empirically for absorption. The unique data with $I \geqslant 2\sigma(I)$ were used to solve and refine the structures. For **3a** measurements were made on a Bruker AXS SMART CCD area-detector diffractometer using graphite-monochromated Mo-Kα radiation ($\lambda = 0.710\ 73$ Å) at 160 ± 2 K. Intensities were corrected semiempirically for absorption.

Structures were solved by direct methods and developed by using alternating cycles of least-squares refinement and Fourier-difference synthesis. All non-hydrogen atoms were refined anisotropically. Hydrogens were generally placed in idealised positions (C–H 0.96 Å) and assigned a common isotropic thermal parameter ($U = 0.08$ Å^2). The hydrogens on the alkenyl ligands and all hydrogens in complex **3a** were located in difference maps. In **3a** there is a disordered diethyl ether molecule. This was modeled with restraints on geometry and anisotropic displacement parameters. Structure solution used SHELXTL PLUS program packages.[38] Selected crystallographic data is given in Table 3.

CCDC reference number 186/2286.

See http://www.rsc.org/suppdata/dt/b0/b007977o/ for crystallographic files in .cif format.

Table 3 Selected crystallographic data for complexes **1a**, **1c**, **2a**, **3a**, **6** and **7**

	1a	**1c**	**2a**	**3a**	**6**	**7**
Formula	$C_{26}H_{17}Fe_2O_6P$	$C_{23}H_{19}Fe_2O_6P$	$C_{26}H_{17}Fe_2O_6P$	$C_{47}H_{42}Fe_2O_6P_2$	$C_{28}H_{26}Fe_2O_8P_2$	$C_{90}H_{105}Fe_6O_{30}P_9$
Formula weight	568.07	534.05	568.07	876.45	664.13	2280.57
Crystal system	Monoclinic	Monoclinic	Monoclinic	Monoclinic	Triclinic	Triclinic
Space group	$P2_1/n$	$P2_1/c$	$P2_1/n$	$P2_1/c$	$P\bar{1}$	$P\bar{1}$
a/Å	14.066(3)	13.444(3)	9.993(2)	16.8886(11)	10.954(2)	11.462(2)
b/Å	12.748(3)	8.120(2)	14.641(3)	12.9963(8)	11.645(2)	17.092(3)
c/Å	14.593(3)	22.698(5)	18.690(4)	19.5996(13)	13.745(2)	27.804(6)
α/°					109.43(3)	80.91(3)
β/°	110.74(3)	91.55(3)	104.49(3)	104.807(2)	99.92(3)	88.26(3)
γ/°					102.79(3)	81.62(3)
V/Å^3	2447.1(9)	2476.9(10)	2647.5(9)	4159.0(5)	1553.7(5)	5321(2)
Z	4	4	4	4	2	2
μ(Mo-Kα)/cm^{-1}	12.90	12.70	11.93	8.23	10.81	10.04
Data measured	4248	4350	4945	25146	5692	11664
Unique data used	4067	4157	4659	9775	5373	10.951
No. parameters	316	289	316	548	361	1216
R (all data)	0.052 (0.123)	0.097 (0.244)	0.049 (0.130)	0.066 (0.128)	0.065 (0.167)	0.071 (0.188)
R_w (all data)	0.089 (0.160)	0.167 (0.342)	0.068 (0.156)	0.115 (0.147)	0.087 (0.195)	0.108 (0.239)

Acknowledgements

We thank the Royal Society for an award allowing O. S. S. to spend a summer at University College, London, Dr Abil E. Aliev (UCL) for help with NMR experiments and Dr Mark Waugh (Newcastle) for synthesis of some starting materials.

References

1 P. M. Maitlis, H. C. Long, R. Quyoum, M. L. Turner and Z.-Q. Wang, *Chem. Commun.*, 1996, 1.

2 S. A. R. Knox, *J. Cluster Sci.*, 1992, **3**, 385; G. C. Bruce, B. Gagnus, S. E. Garner, S. A. R. Knox, A. G. Orpen and A. J. Phillips, *J. Chem. Soc., Chem. Commun.*, 1990, 1360.

3 J. M. Martinez, H. Adams, N. A. Bailey and P. M. Maitlis, *J. Chem. Soc., Chem. Commun.*, 1989, 286; J. Martinez, J. B. Gill, H. Adams, N. A. Bailey, I. M. Saez, G. J. Sunley and P. M. Maitlis, *J. Organomet. Chem.*, 1990, **394**, 583.

4 (*a*) R. Yáñez, J. Ros, X. Solans, M. Font-Altaba and R. Mathieu, *Organometallics*, 1990, **9**, 543; (*b*) R. Yáñez, J. Ros, F. Dahan and R. Mathieu, *Organometallics*, 1990, **9**, 2484.

5 P. O. Nubel and T. L. Brown, *J. Am. Chem. Soc.*, 1982, **104**, 4955; P. O. Nubel and T. L. Brown, *J. Am. Chem. Soc.*, 1984, **106**, 644; P. O. Nubel and T. L. Brown, *J. Am. Chem. Soc.*, 1984, **106**, 3474; P. O. Nubel and T. L. Brown, *J. Am. Chem. Soc.*, 1982, **104**, 4955.

6 G. Hogarth and M. H. Lavender, *J. Chem. Soc., Dalton Trans.*, 1994, 3389.

7 A. F. Dyke, S. A. R. Knox, M. J. Morris and P. J. Naish, *J. Chem. Soc., Dalton Trans.*, 1983, 1417.

8 N. J. Forrow and S. A. R. Knox, unpublished results as quoted in ref. 7.

9 G. Hogarth and M. H. Lavender, *J. Chem. Soc., Dalton Trans.*, 1992, 2759.

10 G. Hogarth, M. H. Lavender and K. Shukri, *Organometallics*, 1995, **14**, 2325.

11 S. A. MacLaughlin, S. Doherty, N. J. Taylor and A. J. Carty, *Organometallics*, 1992, **11**, 4315.

12 G. Hogarth, K. Shukri, S. Doherty, A. J. Carty and G. D. Enright, *Inorg. Chim. Acta*, 1999, **291**, 178.

13 G. Hogarth, M. H. Lavender and K. Shukri, *J. Organomet. Chem.*, 1997, **527**, 247.

14 S. Doherty and G. Hogarth, *Inorg. Chem. Commun.*, 1998, **1**, 257.

15 S. Doherty and G. Hogarth, *Chem. Commun.*, 1998, 1815.

16 R. Yáñez, J. Ros, R. Mathieu, X. Solans and M. Font-Bardia, *J. Organomet. Chem.*, 1990, **389**, 219.

17 G. G. Hlatky and R. H. Crabtree, *Coord. Chem. Rev.*, 1985, **65**, 1.

18 D. S. Moore and S. D. Robinson, *Chem. Soc. Rev.*, 1983, 415.

19 S. Otsuka and A. Nakamura, *Adv. Organomet. Chem.*, 1976, **14**, 245.

20 G. E. Herberich, B. Hessner and J. Okuda, *J. Organomet. Chem.*, 1983, **254**, 317; G. E. Herberich and W. Barlage, *Organometallics*, 1987, **6**, 1924; G. E. Herberich and H. Mayer, *J. Organomet. Chem.*, 1988, **347**, 93; M. Dubeck and R. A. Schell, *Inorg. Chem.*, 1964, **3**, 1757; A. Nakamura and S. Otsuka, *J. Am. Chem. Soc.*, 1972, **94**, 1886.

21 H. C. Clark, G. Ferguson, A. B. Goel, E. G. Janzen, H. Ruegger, P. W. Siew and C. S. Wong, *J. Am. Chem. Soc.*, 1986, **108**, 6961; W. D. Jones, V. L. Chandler and F. J. Feher, *Organometallics*, 1990, **9**, 164.

22 J. D. Vessey and R. W. Mawby, *J. Chem. Soc., Dalton Trans.*, 1993, 51.

23 J. Liu, A. J. Deeming and S. Donovan-Mtunzi, *J. Chem. Soc., Chem. Commun.*, 1984, 1182.

24 R. T. Baker, P. J. Krusic, J. C. Calabrese and D. C. Roe, *Organometallics*, 1986, **5**, 1506.

25 Th. Fässler and G. Huttner, *J. Organomet. Chem.*, 1989, **376**, 367.

26 S. Doherty, G. Hogarth, M. Waugh, T. H. Scanlan, W. Clegg and M. R. J. Elsegood, *Organometallics*, 1999, **18**, 3178; S. Doherty, M. R. J. Elsegood, W. Clegg, M. F. Ward and M. Waugh, *Organometallics*, 1997, **16**, 4251; A. J. Carty, G. M. Mott and N. J. Taylor, *J. Organomet. Chem.*, 1981, **212**, C54.

27 S. Doherty, G. Hogarth, M. R. J. Elsegood, W. Clegg, N. H. Rees and M. Waugh, *Organometallics*, 1998, **17**, 3331.

28 Y. Xin-Kan, W. Ru-Ji, W. Hong-Gen, S. Li-Cheng, H. Qing-Mei and W. Ji-Tao, *Acta Crystallogr., Sect. C*, 1989, **45**, 575.

29 R. Yáñez, J. Ros, X. Solans and M. Font-Bardia, *J. Organomet. Chem.*, 1990, **395**, 305.

30 R. Reina, O. Rossell, M. Seco, J. Ros, R. Yáñez and A. Perales, *Inorg. Chem.*, 1991, **30**, 3973.

31 J. Ros, J. M. Vinas, R. Mathieu, X. Solans and M. Font-Bardia, *J. Chem. Soc., Dalton Trans.*, 1988, 281.

32 A. Ibbotson, A. C. Reduto dos Reis, S. P. Saberi, A. M. Z. Slawin, S. E. Thomas, G. J. Tustin and D. J. Williams, *J. Chem. Soc., Perkin Trans. 1*, 1992, 1251.

33 X.-K. Yao, R.-J. Wang, H.-G. Wang, L.-S. Song, Q.-M. Hu and J.-T. Wang, *Acta Crystallogr., Sect. C*, 1989, **45**, 1989.

34 J. Ros, J. M. Vinas, R. Mathieu, X. Solans and M. Font-Bardia, *J. Organomet. Chem.*, 1986, **307**, C7.

35 D. Seyferth, L. L. Anderson, F. Villãfane, M. Cowie and R. W. Hilts, *Organometallics*, 1992, **11**, 3262.

36 L.-S. Song, C.-G. Yan, Q.-M. Hu, R.-J. Wang and H.-G. Wang, *Huaxue Xuebao*, 1995, **53**, 402.

37 W. T. Osterloh, Ph.D. Thesis, University of Texas, Austin, 1982; R. T. Baker, J. C. Calabrese, P. J. Krusig, M. J. Therien and W. C. Trogler, *J. Am. Chem. Soc.*, 1988, **110**, 8392.

38 G. M. Sheldrick, SHELXTL PLUS, program package for structure solution and refinement, version 4.2, Siemens Analytical Instruments Inc., Madison, WI, 1990.